JOC The Journal of Organic Chemistry

Article

Azulichlorins and Benzocarbachlorins Derived Therefrom

Mario A Noboa, Deyaa I. AbuSalim, and Timothy D. Lash

J. Org. Chem., **Just Accepted Manuscript** • DOI: 10.1021/acs.joc.9b01578 • Publication Date (Web): 20 Aug 2019

Azulichlorins and Benzocarbachlorins Derived Therefrom

Mario A. Noboa, Deyaa I. AbuSalim and Timothy D. Lash*

Department of Chemistry, Illinois State University, Normal, Illinois 61790-4160

E-mail: tdlash@ilstu.edu

Abstract

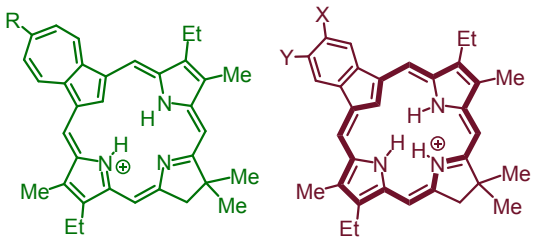

R = H or t-Bu X,Y = H or CHO

Acid-catalyzed condensation of azulidipyrrane aldehydes with a dihydrodipyrrin carbaldehyde afforded the first examples of azulichlorins. These macrocyclic products were isolated in a monoprotonated form, and the free bases proved to be somewhat unstable. The monocations were strongly diatropic and proton NMR spectroscopy showed the internal C-H at ca. -2 ppm. Addition of TFA gave the related dications, but these exhibited significantly reduced aromatic ring currents. Reaction of an azulichlorin with *tert*-butyl hydroperoxide and KOH in dichloromethane-methanol gave a benzocarbachlorin and two related aldehydes. The UV-vis spectrum for the benzocarbachlorin showed a split Soret band at 414 and 430 nm, together with a strong chlorin-like absorption at 684 nm. The proton NMR spectrum indicated that the carbachlorin is strongly aromatic and the internal C-H was observed at -4.64 ppm. Addition of TFA afforded a C-protonated dication with a significantly increased diatropic ring current. The proton NMR spectrum, NICS calculations and AICD plots indicated that the system favors a 22π electron delocalization pathway that runs through the fused benzo-unit. Addition of TFA to the benzocarbachlorin aldehydes primarily led to the formation of monocations, and the generation of C-protonated dications was no longer favored due to the presence of electron-withdrawing formyl moieties.

Introduction

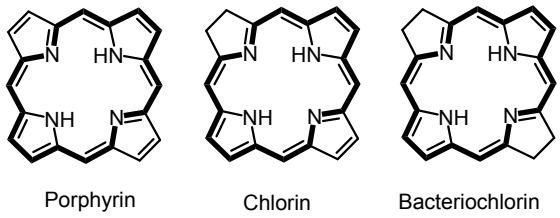

Figure 1. Structures of porphyrin, chlorin and bacteriochlorin.

Hydroporphyrins such as chlorins and bacteriochlorins (Figure 1) are widespread in nature and fulfill many important functions.[1-3] Most of the chlorophylls are magnesium chlorins,[3] while many bacteria utilize the iron(II) chlorin heme d (**1**, Figure 2) in the reduction of molecular oxygen to water.[4] Bacteriochlorophylls *a* and *b* are magnesium bacteriochlorins, and tolyporphin,[5] heme d_1,[6] and siroheme[7] are examples of isobacterichlorins. In addition, the marine worm *Bonellia viridis* generates the *gem*-dimethylchlorin bonellin (**2**) and this green pigment directs masculization of the larvae.[8] Bonellin also exhibits antitumor activity[9] and chlorophyll-derived chlorins isolated from diatoms, sponges, tunicates and mollusks have been shown to have antioxidant properties.[10] Chlorins have comparatively long wavelength absorptions near 650 nm, an attribute that is valued in the development of superior photosensitizers for applications in photodynamic therapy (PDT). For instance, Verteporfin (Visudyne, **3**) is a photosensitizer that has been used to treat age-related macular degeneration[11] and has also been shown to have potential in atheroschlerotic plaque therapy.[12] *meso*-Tetrakis(3-hydroxyphenyl)chlorin (Temoporfin) is similarly being used to treat squamous cell carcinomas,[13] and Talaporfin (**4**) is being applied to the treatment of lung cancer.[14] Unsurprisingly, chlorins have been widely investigated and many synthetic routes to this system have been developed.[1,2,15] However, closely related chlorin-like

systems have not been well studied even though these have the potential to possess equally valuable properties.[16]

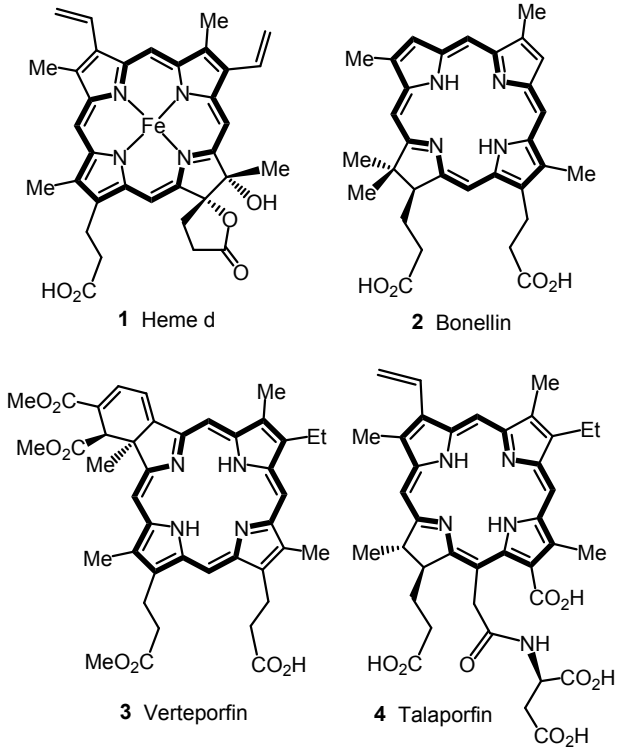

Figure 2. Examples of biologically active chlorins.

Carbaporphyrinoid systems, where one or more of the core nitrogens within the porphyrin macrocycle have been replaced by carbon atoms, have diverse structural and spectroscopic properties[17] and display unusual reactivity such as the capacity to generate stable organometallic derivatives.[18] Examples of 2,3-dihydrocarbaporphyrins such as **5**-**8** (Figure 3) have been reported[19-22] and these chlorin analogues all have strongly aromatic properties. In common with true chlorins, carbachlorins **5**-**8** show moderately strong absorptions near 650 nm, but are relatively stable compounds compared to the tetrapyrrolic structures. Carbachlorins **5** and **8** only undergo oxidation to carbaporphyrins when heated with DDQ in toluene,[20,21] while the five-membered ring fused carbachlorins **6** resisted oxidation under any of the conditions examined.[19] This process is

blocked altogether in the *gem*-diester **7**.[21] It is noteworthy that these structures only represent a single category of carbachlorin where the carbocyclic ring has been reduced. Carbachlorins **CC-c** and **CC-b** with reductions of pyrrole rings c and b, respectively, represent currently unknown examples of chlorin analogues, and the related benzocarbachlorins **BCC-c** and **BCC-b** have also hitherto not been explored (Figure 4). In addition, dihydroazuliporphyrins **AzC-c** and **AzC-b** are examples of previously unknown azulichlorin structures.

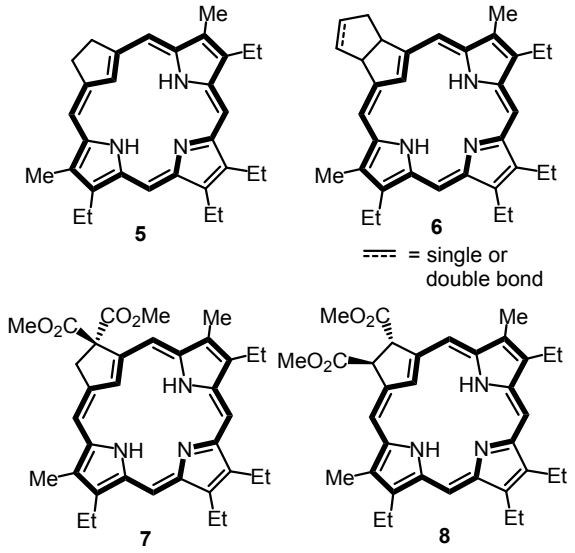

Figure 3. Previously reported carbachlorins.

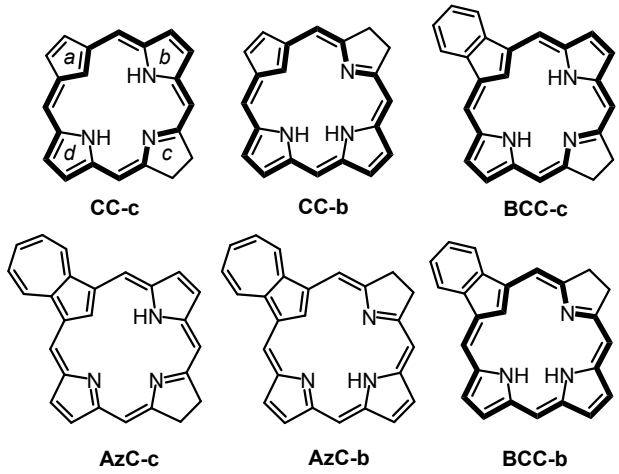

Figure 4. Proposed carbachlorin and azulichlorin systems.

Azuliporphyrins **9** are porphyrin analogues that have an azulene unit instead of one of the pyrrole rings (Figure 5).[23] This system acts as a dianionic ligand and affords organometallic derivatives with Ni(II),[24] Pd(II),[24] Pt(II),[24] Ru(II),[25] Rh(III)[26] and Ir(III).[27] The first example of an azuliporphyrin was reported in 1997,[28] and this system was shown to have significantly reduced diatropic properties compared to porphyrins or carbaporphyrins.[29] The intriguing reactivity and spectroscopic properties of azuliporphyrins has led to the investigation of related porphyrinoid structures, including azulicorrole **10**,[30] azulisapphyrin **11**,[31] and the azulene-fused aza-coronene analogue **12**.[32] Hence, the development of syntheses for azulichlorins and new classes of carbachlorins was considered to be desirable for the development of this field. In this paper, syntheses of azulichlorins belonging to the **AzC-c** class and related benzocarbachlorins belonging to category **BCC-c**, are reported and detailed spectroscopic and computational studies have been performed.[33]

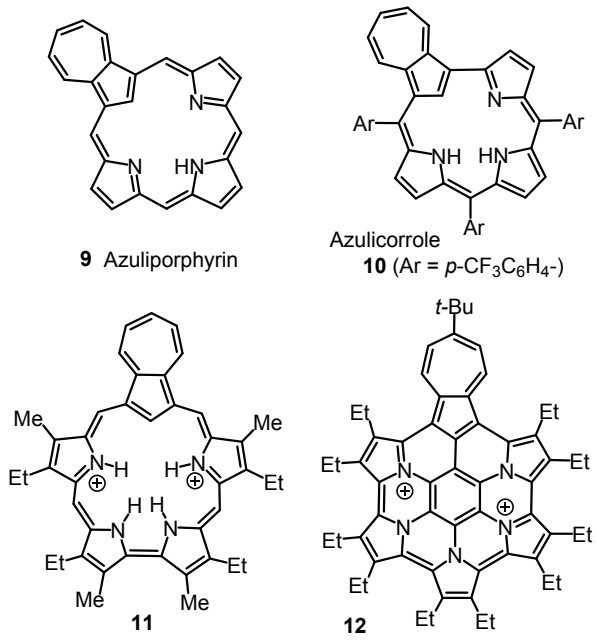

Figure 5. Examples of azulene-containing porphyrin analogues.

Results and Discussion

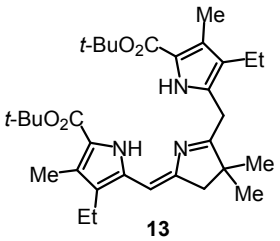

13

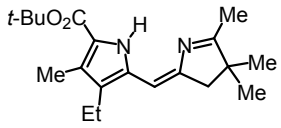

14

The '3 + 1' version of the MacDonald condensation is a versatile method for preparing diverse porphyrinoid structures.[34] Initially, dihydrotripyrrene **13** was targeted as a potential intermediate in the synthesis of carbachlorin analogues. In principle, cleavage of the *tert*-butyl ester protective groups, followed by condensation with monocyclic dialdehydes, would afford the desired macrocyclic products. Convenient syntheses of dihydrodipyrrins related to structure **14** have been reported by Jacobi and coworkers,[35-38] and these useful intermediates have been used to prepare a variety of chlorin[37,38] and bacteriochlorin products.[39] It was anticipated that functionalization of the terminal methyl unit in **14**, followed by condensation with an α-unsubstitued pyrrole, would afford the required dihydrotripyrrene.

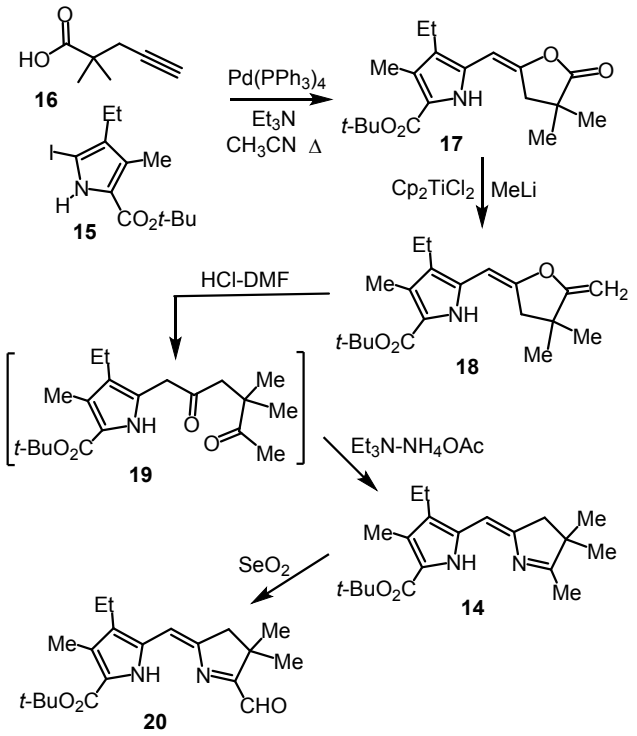

Scheme 1. Synthesis of dihydrodipyrrin intermediates.

Heck coupling of iodopyrrole **15** with pentynoic acid **16** and catalytic $Pd(PPh_3)_4$ in refluxing triethylamine-acetonitrile gave lactone **17** in 87% yield (Scheme 1). The formation of *Z*-isomer **17** was confirmed by NOE difference proton NMR spectroscopy. These studies showed interactions between the N-H resonance and the lactone CH_2 unit that would only be observed in the *Z*-isomer. Furthermore, the bridge C-H weakly interacted with the CH_2 resonance for the ethyl substituent. Reaction of **17** with the Petasis reagent (dimethyl titanocene) in refluxing toluene afforded the related enol ether **18** in 76% yield. NOE difference proton NMR spectroscopy again confirmed that the *Z*-isomer had been obtained. The two protons attached to the exocyclic double bond gave 1H doublets at 4.02 and 4.40 ppm, and the upfield resonance was shown to correspond to the hydrogen atom that was orientated towards the *gem*-dimethyl unit. In a one-pot procedure, enol ether **18** was dissolved in DMF and hydrolyzed with 6 M hydrochloric acid to generate diketone

19. This intermediate underwent a Paal-Knorr cyclization *in situ* with excess ammonium acetate and triethylamine at 55 °C, and following purification by flash chromatography on silica gel, dihydrodipyrrin **14** was isolated in 70% yield (Scheme 1). This product was shown to take on the desired *E*-geometry by NOE difference proton NMR spectroscopy as the resonance for the bridge C-H at 5.82 ppm correlated with the pyrrolene methylene unit at 2.58 ppm.

Attempts to functionalize the terminal methyl group of **14** with lead tetraacetate, *N*-bromosuccinimide, *N*-iodosuccinimide, or *N*-chlorosuccinimide led to decomposition. Jacobi had reported that related dihydrodipyrrins could be selectively oxidized with selenium dioxide to give aldehydes **20** and this transformation proved to be successful for **14** as well. Reaction of **14** with one equivalent of selenium dioxide in DMF-pyridine, followed by purification using flash chromatography (silica gel, eluting with toluene) gave aldehyde **20** in 46% yield (Scheme 1). However, the formyl unit could not be reduced without destroying the dihydrodipyrrin, presumably due to the presence of a reactive imine unit.

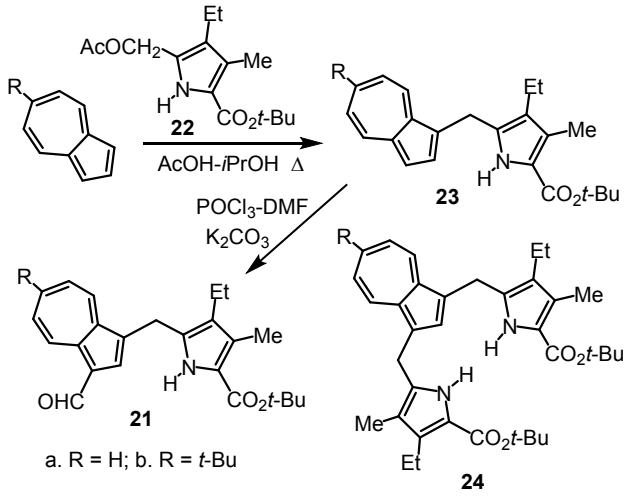

Scheme 2. Synthesis of azulidipyrrane carbaldehydes.

Given the difficulties that had been encountered, it was necessary to develop an alternative strategy for the synthesis of carbachlorin-type structures such as azulichlorins **AzC-c**. As dihydropyrrin monoaldehyde was readily available, an alternative '2 + 2' strategy was designed that made use of this intermediate. This necessitated the use of complementary azulidipyrrane aldehydes **21**. (Scheme 2). Azulene was reacted with one equivalent of acetoxymethylpyrrole **22** and acetic acid in refluxing isopropyl alcohol. Following column chromatography, azulidipyrrane **23a** was obtained as the major product, together with the related azulitripyrrane **24a**.[40,41] Condensation of 6-*tert*-butylazulene with **22** similarly gave azulidipyrrane **23b**, together with azulitripyrrane **24b** (Scheme 2). Initially, formylation of **23a** or **23b** using the Vilsmeier-Haack reaction ($POCl_3$-DMF) gave poor results because the acidic conditions cleaved the *tert*-butyl ester protective groups. However, when the reaction of **23a** was carried out in the presence of potassium carbonate, azulidipyrrane aldehyde **21a** was generated in 69% yield. Azulidipyrrane **23b** reacted similarly to afford the related aldehyde **21b** (Scheme 2).

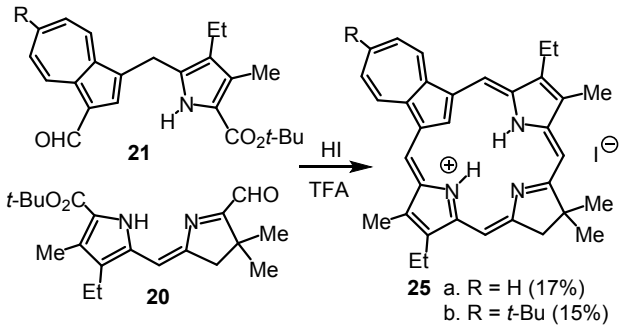

Scheme 3. Synthesis of azulichlorins.

Aldehydes **20** and **21a** were treated with TFA to cleave the *tert*-butyl ester protective groups, and the solutions were then diluted with acetic acid and further acidified with hydroiodic acid (Scheme 3). Although self-condensation of **20** or **21a** could potentially occur, only one macrocyclic product was identified resulting from the desired cross-condensation reaction. The

reaction mixture was stirred at room temperature overnight, and the product purified on a silica gel column. A green band was collected and further purified on a basic alumina column to give the monoprotonated azulichlorin **25a**.HI in 17% yield. The proton NMR spectrum for **25a**H^+ in $CDCl_3$ (Figure 6) shows the internal C-H proton at -2.11 ppm, and this result indicates that the monocation has a similar diamagnetic ring current to protonated azuliporphyrins. The *meso*-protons were shifted downfield to give four singlets at 7.51 (10-H), 7.58 (15-H), 9.22 (20-H) and 9.28 (5-H) ppm.

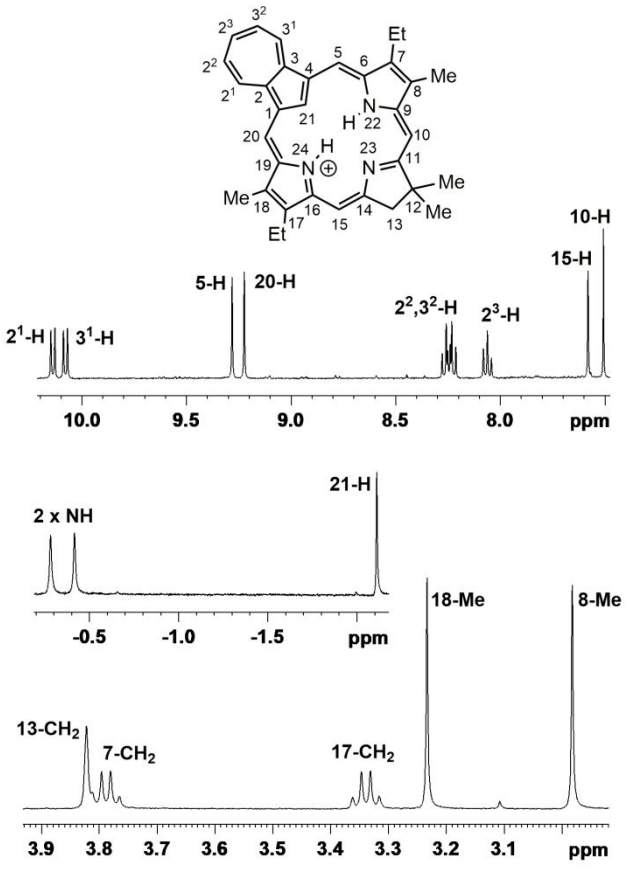

Figure 6. Proton NMR spectrum of azulichlorin **25a**.HI in $CDCl_3$.

The UV-Vis spectrum of azulichlorin **25a**H^+ gave a strong Soret band at 445 nm along with two weaker broad bands at 620 and 670 nm (Figure 7). When **25aH**$^+$ was exposed to triethylamine, a

yellow solution corresponding to the free base azulichlorin **25a** was generated (Scheme 4). The UV-vis spectrum of **25a** in 1% Et_3N-chloroform (Figure 7) showed substantial changes and the Soret band was lost, suggesting a decrease in aromaticity. The free-base form is somewhat unstable and slowly air oxidized to give impure carbachlorins. The proton NMR spectra of **25a** in Et_3N-$CDCl_3$ or d_5-pyridine gave broad poorly resolved peaks. Addition of TFA afforded a diprotonated species **25a**H_2^{2+} and the resulting UV-vis spectrum in 5% TFA-chloroform showed a strong Soret band at 457 nm and weaker absorptions at 345, 505, 605 and 645 nm (Figure 7). Interestingly, the proton NMR spectrum of **25a**H_2^{2+} showed a decrease in diatropic ring current compared to the mono-protonated species as the internal C-H proton was only shifted upfield to 2.24 ppm, while the NH protons gave broad peaks at 1.26, 5.40 and 5.41 ppm. The *meso*-protons, however, were less affected, showing only a minor shifts compared to **25a**H^+.

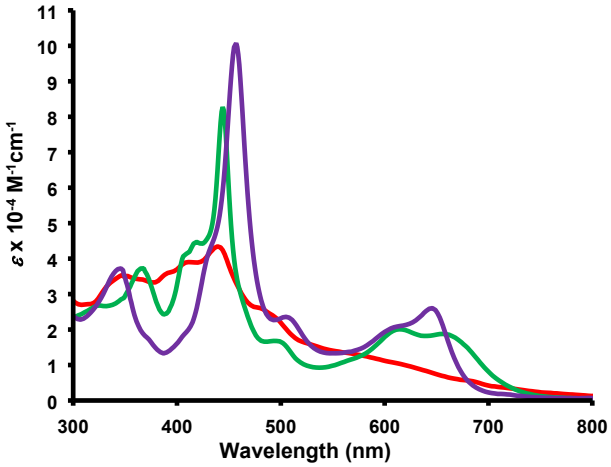

Figure 7. UV-vis spectra of azulichlorin **25a** in 1% Et_3N-$CHCl_3$ (free base, red line), $CHCl_3$ (monocation **25a**H^+, green line) and 5% TFA-$CHCl_3$ (dication **25a**H_2^{2+}, purple line).

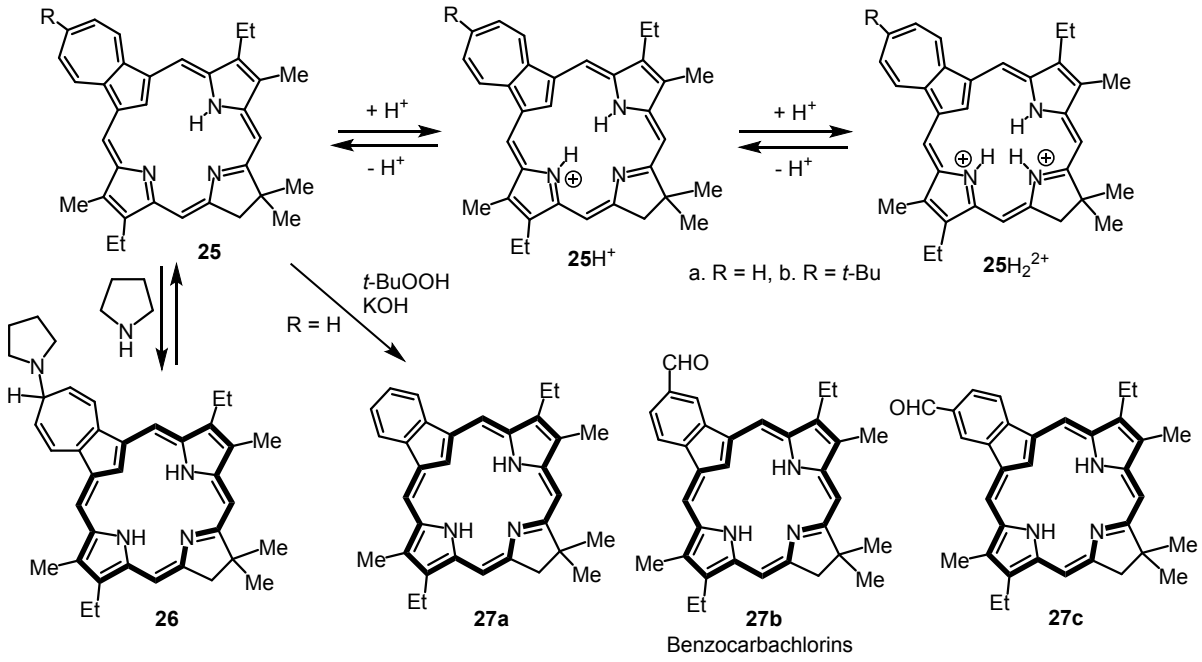

Scheme 4. Protonation of azulichlorins and ring contraction to give benzocarbachlorins.

tert-Butylazulichlorin **25b** was synthesized under the same conditions from azulidipyrrane aldehyde **21b** and dihydrodipyrrin aldehyde **20**. As expected, azulichlorin **25b** was isolated as the monoprotonated species and gave a similar UV-vis spectrum to **25a**. The proton NMR spectrum for **25b**H^+ showed substantial diatropic character, although the internal C-H proton was slightly less shielded than the equivalent peak for **25a**H^+ and appeared at -1.46 ppm. However, the *meso*-protons were significantly deshielded compared to **25a**H, giving rise to four 1H singlets at 7.72, 7.83, 9.60 and 9.65 ppm. On balance, the presence of the *tert*-butyl substituent appears to enhance the diatropicity of the macrocycle. Similar observations were previously reported for *tert*-butyl substituted azuliporphyrins.[41]

Azuliporphyrins are susceptible to nucleophilic attack on the seven-membered ring and addition of pyrrolidine results in the reversible formation of aromatic carbaporphyrin adducts.[23,42] Addition of pyrrolidine to a solution of **25a**.HI gave a UV-vis spectrum that resembled an aromatic

porphyrinoid structure. Specifically, a strong Soret band was observed at 408 nm and a moderately strong chlorin-like absorption appeared at 677 nm (Figure 8). The proton NMR spectrum of **25a** with pyrrolidine in $CDCl_3$ showed the formation of a strongly aromatic species. The internal C-H was shifted upfied to -4.59 ppm and two broad NH resonances were observed at -2.16 and -2.12 ppm. The *meso*-protons were shifted downfield to give four 1H singlets at 8.34, 8.45, 9.49 and 9.52 ppm, and the resonances for the methyl substituents were also further deshielded giving rise to two 3H singlets at 3.27 and 3.36 ppm. The cycloheptatriene unit gave a 2H doublet at 7.70 and a 2H multiplet at 5.92-5.96 ppm. The results are consistent with the formation of the pyrrolidine adduct **26** where nucleophilic attack is favored at position 2[3] (Scheme 4). The reduced 13-CH_2 unit afforded an AB quartet ($^2J_{HH}$ = 16.3 Hz) for 2H at 4.39-4.47 ppm. This arises because the presence of the pyrrolidine unit differentiates the two faces of the macrocycle, and this leads to geminal coupling between the two protons.

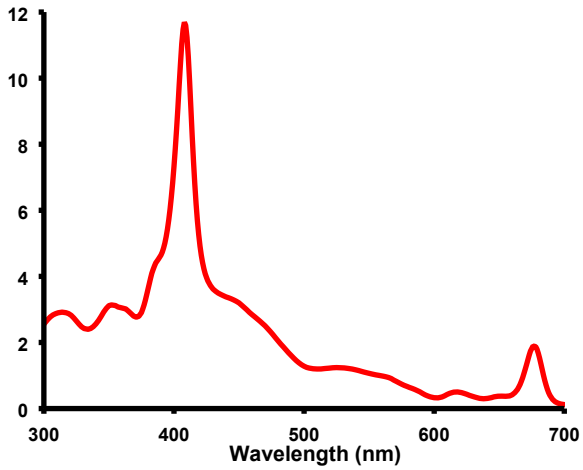

Figure 8. UV-vis spectrum of azulichlorin **25a** in 1% pyrrolidine-$CHCl_3$ showing the formation of carbachlorin adduct **26**.

In earlier work, azuliporphyrins had been reported to undergo oxidative ring contractions to generate benzocarbaporphyrins[42,43] and it was proposed that this transformation was triggered by

initial nucleophilic attack onto the seven-membered ring. In a typical procedure, azuliporphyrins were reacted with *tert*-butyl hydroperoxide and KOH at room temperature. The same synthetic methodology was used to convert azulichlorin **25a** into the first examples of benzocarbachlorins (Scheme 4). Azulichlorin **25a** was reacted with potassium hydroxide and *tert*-butyl hydroperoxide in dichloromethane-methanol at room temperature. Following work up, the residue was chromatographed on a grade 3 alumina column, eluting initially with 30% dichloromethane-hexanes, and an orange band was collected. Following recrystallization from chloroform-hexanes, benzocarbachlorin **27a** was obtained in 24% yield as a yellow-brown powder. A second major orange band was collected corresponding to a mixture of two isomeric benzocarbachlorin aldehydes **27b** and **27c** in 37-46% yield (Scheme 4).

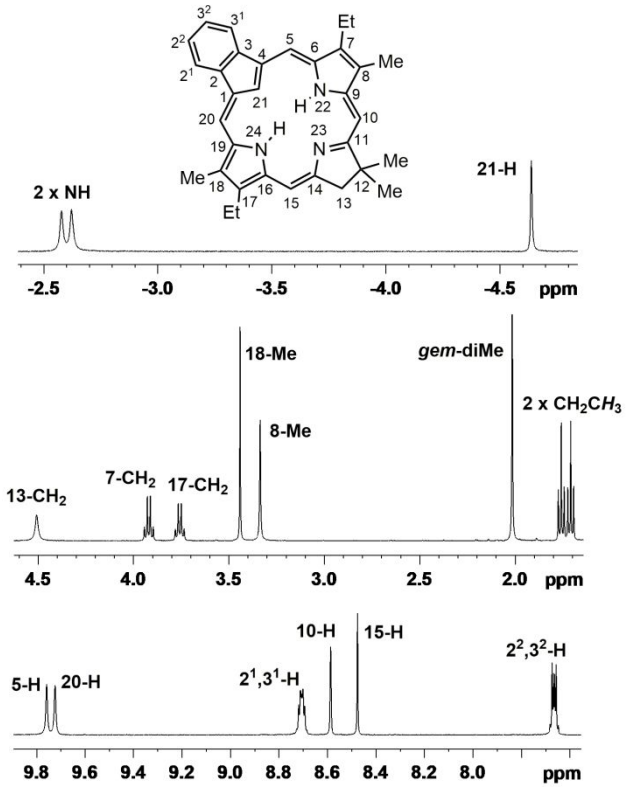

Figure 9. Proton NMR spectrum of benzocarbachlorin **27a** in $CDCl_3$.

The proton NMR spectrum for benzocarbachlorin **27a** in $CDCl_3$ showed the presence of a strong diamagnetic ring current (Figure 9). The internal C-H proton was observed at -4.64 ppm and the N-H protons gave broad peaks at -2.63 and -2.58 ppm. The external *meso*-protons were shifted downfield to give four 1H singlets at 8.47 (10-H), 8.59 (15-H), 9.72 (20-H) and 9.76 (5-H) ppm. The carbon-13 NMR spectrum showed the internal CH at 111.4 ppm, while the *meso*-carbons appeared at 90.2 (C-10), 92.1 (C-15), 101.3 (C-20) and 101.6 (C-5) ppm. The UV-vis spectrum of benzocarbachlorin **27a** in 1% Et_3N-chloroform produced a split Soret band at 414 and 430 nm, together with a strong absorption at 684 nm that is characteristic of chlorin-type structures (Figure 10).

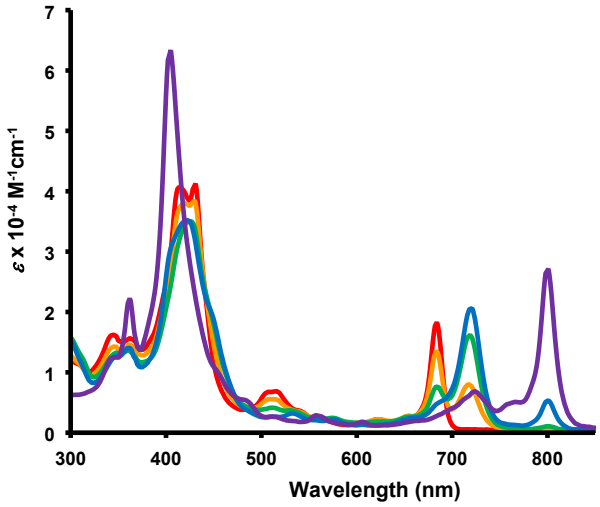

Figure 10. UV-vis spectra of benzocarbachlorin in $CHCl_3$ (free base, red line), 0.1% TFA-$CHCl_3$ (orange line), 0.2% TFA-$CHCl_3$ (green line), 0.5% TFA-$CHCl_3$ (blue line), and 5% TFA-$CHCl_3$ (dication **27a**H_2^{2+}, purple line).

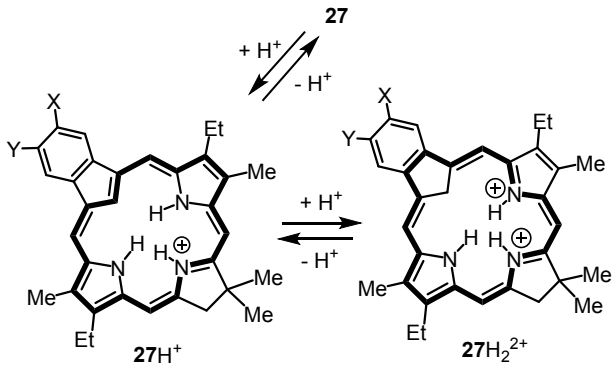

a. X = Y = H; b. X = CHO, Y = H; c. X = H, Y = CHO

Scheme 5. Protonation of benzocarbachlorins.

Addition of small amounts of TFA generated a monocationic species **27a**H^+ (Scheme 5). The UV-spectrum for a solution of **27a** with 0.1% TFA/$CHCl_3$ showed that a new species had been partially formed as a new absorption band had emerged at 717 nm. In 0.2% TFA-chloroform, this species predominated but a new band started to emerge at 800 nm. In 5% TFA-chloroform, the carbachlorin was completely converted into the latter form, and this was assigned to the dicationic structure **27a**H_2^{2+}. The dication gave a strong Soret band at 404 nm, in addition to the long wavelength absorption at 800 nm (Figure 10). The proton NMR spectrum for dication **27a**H_2^{2+} in TFA-$CDCl_3$ confirmed that C-protonation had occurred, and indicated that the diatropicity of the carbachlorin system had been increased. The internal CH_2 resonance was observed upfield at -6.77 ppm, while the *meso*-protons were shifted downfield to give singlets at 9.47, 9.64, 11.120 and 11.126 ppm. The chemical shifts for the methyl substituents were also shifted downfield by ca. 0.26 ppm, which also implies that a larger macrocyclic ring current is present. Major changes were observed for the chemical shifts of the benzo-protons. In the free base form, the 2^1,3^1-protons gave a multiplet at 8.68-8.73 ppm and the 2^2,3^2-protons appeared at 7.65-7.68 ppm, but these resonances were shifted downfield for **27a**H_2^{2+} to give multiplets at 10.09-10.12 ppm and 8.74-8.78 ppm, respectively. These shifts indicate that the global ring current passes through the benzene ring and

indicates that a 22π electron pathway plays a significant role (see computational results below). Similar conjugation pathways have been postulated for protonated benzocarbaporphyrins and naphthocarbaporphyrins.[44,45] The carbon-13 NMR spectrum for **27a**H_2^{2+} showed the internal CH_2 at 32.0 ppm, while the *meso*-carbons appeared at 101.2, 103.2 and 105.8 ppm (the latter resonance corresponds to both the 5- and 20-CHs).

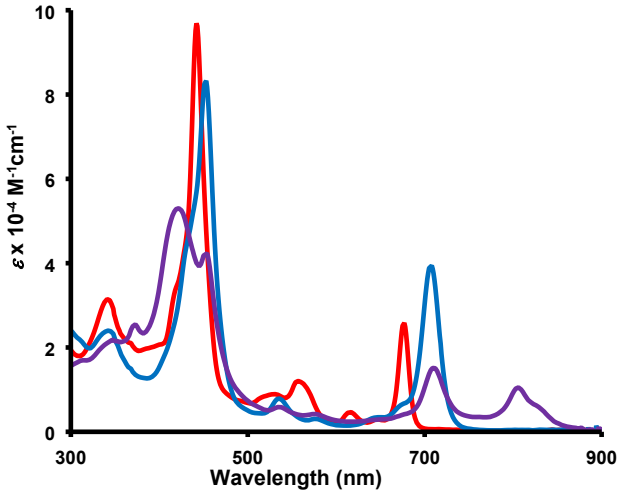

Figure 11. UV-vis spectra of benzocarbachlorincarbaldehydes **27b,c** in $CHCl_3$ (free bases, red line), 1% TFA- $CHCl_3$ (monocations **27b,c**H^+, blue line), and 50% TFA-$CHCl_3$ (mixture of monocations **27b,c**H^+ and dications **27b,c**H_2^{2+}, purple line).

Attempts to separate benzocarbachlorin aldehydes **27b** and **27c** were unsuccessful, and spectroscopic characterization was performed on the isomeric mixture. The proton NMR spectrum of **27b,c** in $CDCl_3$ showed that the two isomers were present in a 50/50 mixture, and both forms showed the presence of strong diamagnetic ring currents. The internal C-H protons were observed at -4.70 and -4.69 ppm, while the *meso*-protons gave rise to a series of singlets between 8.43 and 9.55 ppm. The aldehyde protons gave a singlet at 10.28 ppm. The UV-vis spectrum of **27b,c** gave a strong Soret band at 442 nm, together with small Q bands at 530, 557 and 616 nm and a stronger chlorin-type absorption at 676 nm (Figure 11). In 0.1% TFA-$CHCl_3$ a new species was formed

that afforded a Soret band at 450 nm and a strong absorption at 707 nm, and this was assigned to monocation **27b,c**H^+ (Scheme 5). However, further addition of TFA did not initially show any significant changes. Benzocarbachlorin **27a** was completely converted into the dicationic species **27a**H_2^{2+} in 5% TFA-$CHCl_3$, but benzocarbachlorins **27a,b** only showed trace amounts of the related dications in 10% TFA-chloroform (Figure 11). Even in 50% TFA-chloroform solutions, conversion to **27b,c**H_2^{2+} was incomplete. The presence of electron-withdrawing groups on the benzene ring apparently inhibits the second protonation step, indicating that there must be a significant electronic interaction between the benzo-unit and the porphyrinoid macrocycle in these dicationic structures. This differs from the free base and monocationic forms, where the benzo-units appear to be effectively disconnected from the macrocyclic π-system. The proton NMR spectrum of **27b,c**H^+ in $CDCl_3$ containing a trace amount of TFA showed a downfield shift to the internal C-H protons from -4.7 ppm to -2.0 ppm, and the *meso*-protons gave rise to singlets between 7.96 and 9.67 ppm. These results indicate that the macrocyclic ring current for the free base and monoprotonated porphyrinoids are very similar. The aldehyde moiety afforded a singlet at 10.20 ppm.

Computational studies were also conducted on unsubstituted azulichlorins **AzC-c** and benzocarbachlorins **BCC-c** and these provide further insights into these novel chlorin analogues. A series of tautomers were examined for the free base and protonated forms for each system. The structures were optimized using B3LYP with the triple-ζ basis set 6-311++G(d,p).[46] Four tautomers for the free base forms of **AzC-c** were considered and these are designated according to the position of the proton as **AzC-c-22H**, **AzC-c-23H**, **AzC-c-5H** and **AzC-c-10H** (Table 1). All four structures are essentially planar. The relative energies were assessed using three different functionals, B3LYP, M06-2X, and B3LYP-D3,[47,48] and the relative Gibbs free energy was

determined using B3LYP. The relative ΔG values were consistently very similar to the relative ΔE values, demonstrating that entropic factors are not significant. The calculations showed that **AzC-c-22H** is the most stable, yet **AzC-c-23H** is only slightly higher in energy. Although the conjugation pathway in **AzC-c-22H**, which passes through an imine unit within the reduced ring, would be expected to be favored over the alternative pathway in **AzC-c-23H** which passes through an amine-type nitrogen, the former species has more steric congestion because the two internal hydrogens are adjacent to one another. The other two tautomers, which have interrupted conjugation pathways due to the presence of methylene bridges, are much higher in energy (Table 1). Nucleus independent chemical shift (NICS) calculations were carried out[49] using CAM-B3LYP to assess the aromatic properties of these structures. Large negative values correspond to highly shielded regions that result from aromatic ring currents, while positive values correspond to deshielded regions. In this study, NICS(0) and $NICS_{zz}(1)$ calculations were conducted. Standard NICS calculations consider the effects due to σ and π electrons and may not always reliably assess aromatic properties, but $NICS_{zz}$ primarily measures the effects due to the π system. $NICS_{zz}$ calculations were performed 1 Å above the ring. It should be noted that the numerical values obtained using $NICS_{zz}(1)$ are much larger than those obtained using NICS(0), but the porphyrinoids examined in these studies showed similar trends using both techniques. To avoid confusion, only the NICS(0) values will be discussed. **AzC-c-22H** exhibits moderate global diatropicity, giving a NICS(0) value of -4.07 ppm. The NICS values for rings *a* and *b* are strongly negative, demonstrating that the ring current primarily runs through the outside of these rings, but rings *c* and *d* give low negative or positive results showing that the pathway runs through the inside of these subunits. In addition to the NICS calculations, anisotropy of induced current density (AICD)[50] was used to assess all of the calculated structures, and the plot for **AzC-c-22H** showed

that bifurcated pathways were present that exclude the cycloheptratriene moiety (Figure 12). The global ring current in **AzC-c-23H** is virtually absent, presumably due to the necessity for this conjugation pathway to pass through the amine-type nitrogen.

Table 1. Calculated Relative Energies (kcal/mol) and NICS Values (ppm) for Free Base Unsubstituted Azulichlorin Tautomers.

	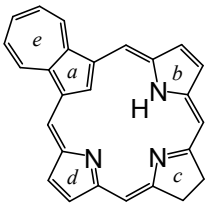	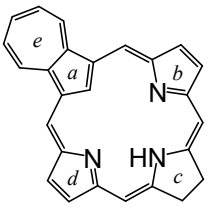	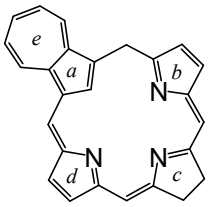	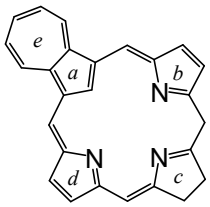
Molecule	**AzC-c-22H**	**AzC-23H**	**AzC-c-5H**	**AzC-10H**
ΔG (298 K)	0.00	+0.12	+28.36	+25.50
ΔE (B3LYP/ **M06-2X**/ B3LYP-D3)	(0.00/ **0.00**/ 0.00)	(-1.27/ **-3.53**/ -1.38)	(+30.23/ **+27.89**/ +30.83)	(+27.00/ **+23.01**/ +27.74)
NICS(0)/NICS(1)$_{zz}$	-4.07/-9.38	-1.69/-2.95	+0.35/+3.27	+1.72/+6.53
NICS(*a*)/NICS(1*a*)$_{zz}$	-14.07/-39.27	-13.46/-38.37	-14.10/-40.59	-13.15/-38.11
NICS(*b*)/NICS(1*b*)$_{zz}$	-6.59/-16.49	-1.36/-9.27	+1.78/-3.74	-1.36/-9.45
NICS(*c*)/NICS(1*c*)$_{zz}$	+3.57/+4.22	+0.54/+4.22	+1.62/+0.02	+1.23/-1.54
NICS(*d*)/NICS(1*d*)$_{zz}$	-0.08/-6.88	-1.36/-9.27	-1.50/-9.66	-0.61/-47.51
NICS(*e*)/NICS(1*e*)$_{zz}$	-0.92/-9.27	-1.90/-11.89	-3.71/-16.09	-3.44/-15.57

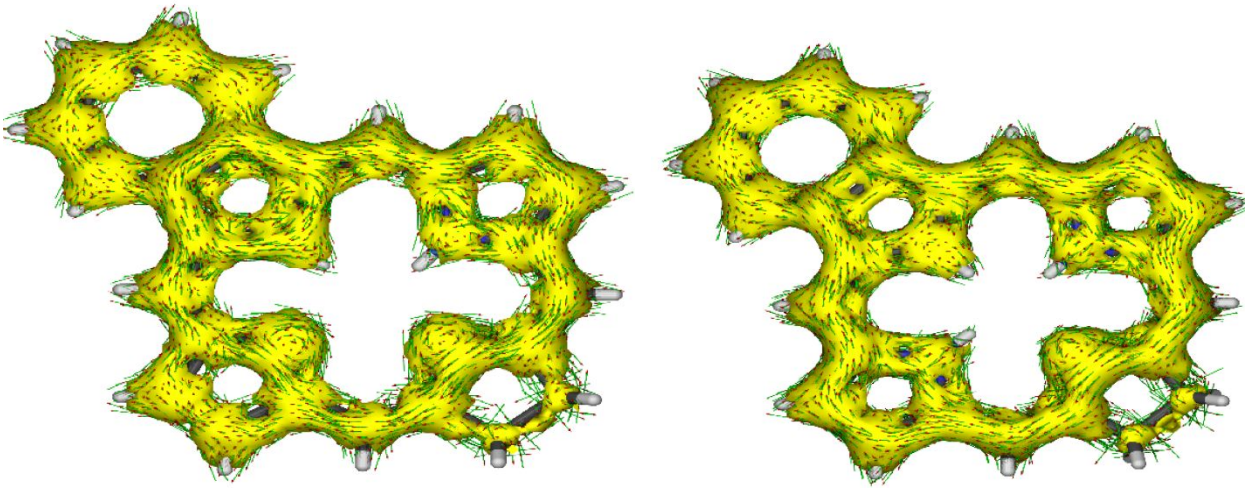

Figure 12. AICD plots (isovalues = 0.05) of azulichlorin **AzC-c-22H** and monocation **AzC-c-22,24H**$^+$.

Table 2. Calculated Relative Energies (kcal/mol) and NICS Values (ppm) for Tautomers of Monoprotonated Azulichlorins.

	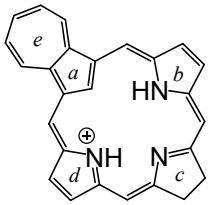	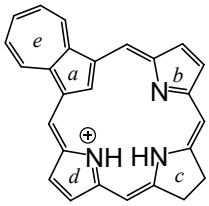	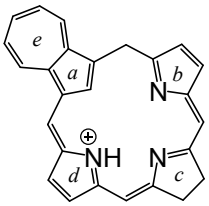	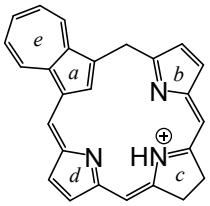
Molecule	**AzC-c-22,24H$^+$**	**AzC-c-22,23H$^+$**	**AzC-c-5,24H$^+$**	**AzC-c-5,23H$^+$**
ΔG (298 K)	0.00	+10.92	+22.55	+31.60
ΔE (B3LYP/ **M06-2X**/ B3LYP-D3)	(0.00/ **0.00**/ 0.00)	(+10.56/ **+9.54**/ +10.73)	(+24.00/ **+22.20**/ +24.92)	(+33.96/ **+34.68**/ +34.76)
NICS(0)/NICS(1)$_{zz}$	-6.85/-17.25	-4.17/-9.82	+0.10/+2.09	-1.92/-3.31
NICS(*a*)/NICS(1*a*)$_{zz}$	-10.76/-28.83	-9.24/-25.74	-9.60/-28.13	-9.48/-28.48
NICS(*b*)/NICS(1*b*)$_{zz}$	-8.30/-20.72	-1.56/-10.51	+2.88/-1.23	+4.00/+0.92
NICS(*c*)/NICS(1*c*)$_{zz}$	+5.00/+5.81	+1.82/+5.52	+1.92/+0.21	+1.93/+5.92
NICS(*d*)/NICS(1*d*)$_{zz}$	-8.31/-20.73	-8.97/-19.50	-7.44/-17.93	-3.16/-13.11
NICS(*e*)/NICS(1*e*)$_{zz}$	-2.91/-16.14	-3.10/-16.43	-4.83/-19.38	-4.00/-17.44
	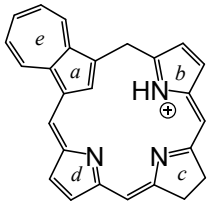	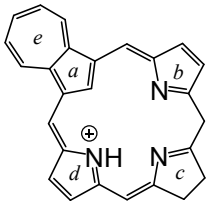	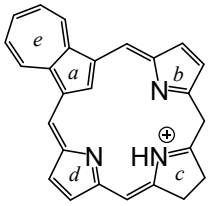	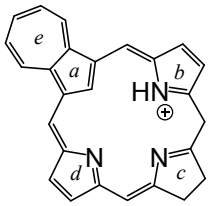
Molecule	**AzC-c-5,22H$^+$**	**AzC-c-10,24H$^+$**	**AzC-c-10,23H$^+$**	**AzC-c-5,22H$^+$**
ΔG (298 K)	+32.35	+20.34	+31.99	+24.75
ΔE (B3LYP/ **M06-2X**/ B3LYP-D3)	(+34.34/ **+37.70**/ +35.27)	(+22.65/ **+20.05**/ +23.68)	(+33.27/ **+30.38**/ +34.26)	(+26.91/ **+24.38**/ +28.02)
NICS(0)/NICS(1)$_{zz}$	-3.29/-6.87	+1.03/+4.47	+0.94/+4.26	+1.20/+4.86
NICS(*a*)/NICS(1*a*)$_{zz}$	-8.49/-26.04	-9.23/-26.98	-9.49/-28.15	-7.83/-23.79
NICS(*b*)/NICS(1*b*)$_{zz}$	-8.89/-21.34	-0.67/-7.73	-3.22/-12.88	-8.32/-19.82
NICS(*c*)/NICS(1*c*)$_{zz}$	+3.74/+4.74	+1.65/-0.92	+0.37/+2.02	+1.59/-0.48
NICS(*d*)/NICS(1*d*)$_{zz}$	-1.19/-9.73	-6.47/-15.59	-2.71/-11.63	+0.83/-4.26
NICS(*e*)/NICS(1*e*)$_{zz}$	-3.78/-17.53	-4.44/-18.53	-4.28/-18.26	-4.45/-18.61

Protonation gives rise to monocationic and dicationic species. Eight possible monocationic tautomers were considered (Table 2), and **AzC-c-22,24H$^+$** was calculated to be by far the most favored form. **AzC-c-22,23H$^+$** was ca. 10 kcal/mol higher in energy, while the remaining *meso*-protonated structures were 22-38 kcal/mol higher in energy. **AzP-c-22,23H$^+$** is less favored due to

steric crowding and the necessity for the π-conjugation pathways to pass through the amine-type nitrogen. Nevertheless, this tautomer has a significant NICS(0) value of -4.17 ppm and therefore would have diatropic character. The favored tautomer, **AzC-c-22,24H**$^+$, gave a larger NICS(0) value of -6.85 ppm and rings *a*, *b* and *d* all gave large negative values, demonstrating that the favored aromatic delocalization pathways run through the outside of these rings. This suggests that the pathway shown in structure **28a** (Figure 13) is favored, although the small negative values calculated for the seven-membered ring (ring *e*) is rather small and therefore not consistent with tropylium character. However, the AICD plot for this tautomer (Figure 12) indicates that π-conjugation extended through the seven-membered ring and instead is suggestive of contributions from 23-atom delocalized structure **28b**. In fact, computational studies on azuliporphyrins also suggest that tropylium character is not favored in the free base and monoprotonated forms,[51] even though this interpretation is generally used to explain the properties of azuliporphyrins.[42] Attempts to rationalize the conjugation pathways in terms of resonance led to the proposal of similar somewhat unlikely canonical forms, and it was concluded that azuliporphyrins cannot be satisfactorily assessed in this fashion.[51] The calculated bond lengths for the favored free base and monocations **AzC-c-22H** and **AzC-c-22,24H**$^+$ showed very little variation for the individual bonds in the seven-membered ring apart from the position for ring fusion. In fact, this bond (C2-C3) was 0.078 Å or 0.067 Å longer, respectively, for these two species. A series of diprotonated dications were also considered (Table 3) and **AzC-c-22,23,24H**$^{2+}$ was unambiguously favored over the C-protonated tautomers. The system retained substantial global diatropicity (NICS(0) = -5.47 ppm), but this is reduced compared to monocation **AzC-22,24H**$^+$ in agreement with the proton NMR spectra obtained for azulichlorins **25a** and **25b**. Rings *a*, *b* and *d* all gave significant negative NICS values, suggesting that the ring current passes through the periphery of these rings. The seven-

membered ring also gives a substantial negative NICS value, potentially indicating that this species possesses tropylium character, and the results are consistent with the conjugation pathway shown in structure **29a** (Figure 13). However, the AICD plot for **AzC-c-22,23,24H^{2+}** (Figure 14) indicates that the global conjugation pathway extends around the periphery of the seven-membered ring. The calculated bond length for C2-C3 is 1.449 Å, which also indicates that this bond has substantial single bond character, although it is slightly shorter than the equivalent bond in **AzC-c-22H**. Again, it is only possible to postulate a rather unconventional resonance contributor **29b** for this species.

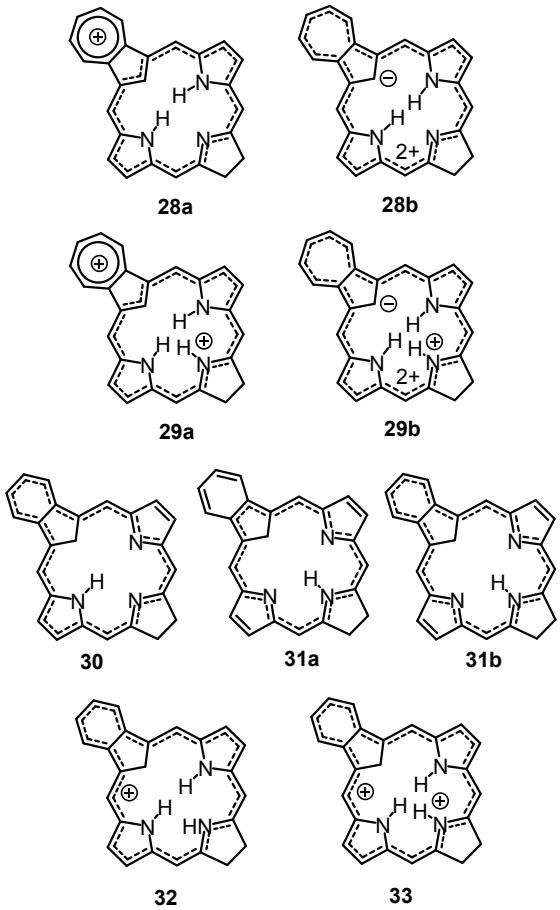

Figure 13. Potential conjugation pathways in selected azulichlorin and benzocarbachlorin structures.

Table 3. Calculated Relative Energies (kcal/mol) and NICS Values (ppm) for Azulichlorin Dications.

	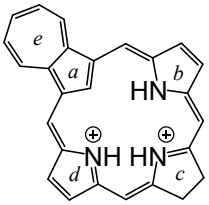	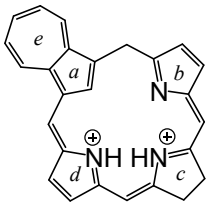	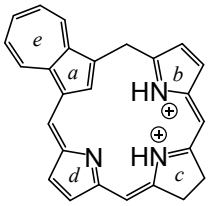	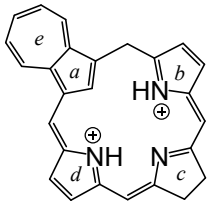
Molecule	**AzC-c-22,23,24H^{2+}**	**AzC-c-5,23,24H^{2+}**	**AzC-c-5,22,23H^{2+}**	**AzC-c-5,22,24H^{2+}**
ΔG (298 K)	0.00	+18.21	+24.61	+10.32
ΔE (B3LYP/ **M06-2X**/ B3LYP-D3)	(0.00/ **0.00**/ 0.00)	(+19.54/ **+18.91**/ +20.50)	(+25.99/ **+30.04**/ +27.01)	(+11.70/ **+14.08**/ +12.59)
NICS(0)/NICS(1)$_{zz}$	-5.47/-8.26	-0.78/-0.07	-3.19/-5.87	-2.71/-4.88
NICS(*a*)/NICS(1*a*)$_{zz}$	-5.58/-16.18	-5.40/-15.85	-0.91/-8.85	-7.05/-19.78
NICS(*b*)/NICS(1*b*)$_{zz}$	-9.48/-18.99	+5.17/+3.94	-10.54/-19.40	-6.15/-15.04
NICS(*c*)/NICS(1*c*)$_{zz}$	+2.85/+4.91	+0.71/+2.90	+2.39/+6.03	+3.22/+3.16
NICS(*d*)/NICS(1*d*)$_{zz}$	-9.48/-18.98	-9.39/-20.02	+1.32/+23.57	-8.54/-20.85
NICS(*e*)/NICS(1*e*)$_{zz}$	-4.12/-19.29	-4.92/-20.83	-4.27/-19.09	-4.80/-20.15
	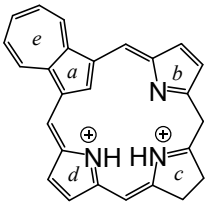	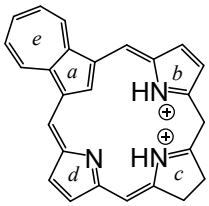	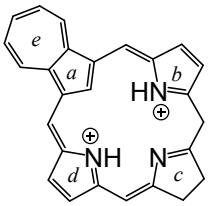	
Molecule	**AzC-c-10,23,24H^{2+}**	**AzC-c-10,22,23H^{2+}**	**AzC-c-10,22,24H^{2+}**	
ΔG (298 K)	+17.72	+21.29	+2.66	
ΔE (B3LYP/ **M06-2X**/ B3LYP-D3)	(+19.09/ **+17.19**/ +20.30)	(+22.57/ **+20.04**/ +23.76)	(+4.04/ **+2.75**/ +5.00)	
NICS(0)/NICS(1)$_{zz}$	+0.76/+3.87	+2.51/+9.20	+0.60/+3.37	
NICS(*a*)/NICS(1*a*)$_{zz}$	-5.19/-14.52	-5.06/-14.59	-7.05/-17.80	
NICS(*b*)/NICS(1*b*)$_{zz}$	-2.21/-11.00	-8.92/-17.83	-5.13/-12.88	
NICS(*c*)/NICS(1*c*)$_{zz}$	+0.10/+1.28	-1.12/-1.27	+1.88/0.00	
NICS(*d*)/NICS(1*d*)$_{zz}$	-8.60/-18.83	-0.77/-7.34	-7.81/-18.45	
NICS(*e*)/NICS(1*e*)$_{zz}$	-5.00/-20.95	-5.40/-21.97	-5.13/-21.35	

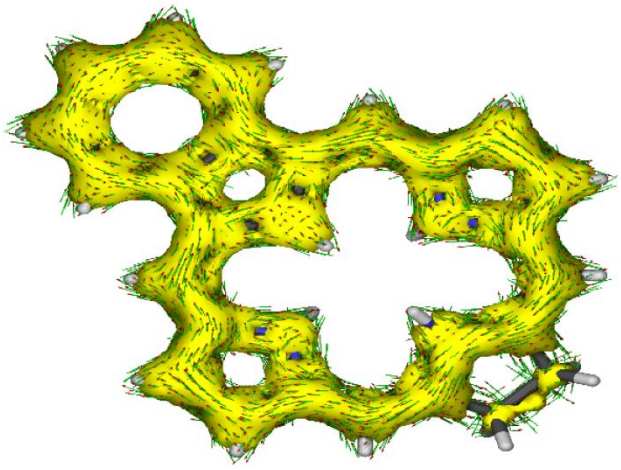

Figure 14. AICD plot (isovalue = 0.05) of azulichlorin dication **AzC-c-22,23,24H**$^{2+}$.

Eight tautomers of free base benzocarbachlorin **BCC-c** were considered and unsurprisingly **BCC-c-22,24H** was the most favored (Table 4). This tautomer is highly diatropic (NICS(0) = -11.70 ppm) and the rings *b* and *c* give large negative NICS values that demonstrate that the macrocyclic ring current runs around the outside of these rings taking the inside track for rings *a* and *c*. This interpretation is confirmed by the AICD plot for this tautomer (Figure 15). Nonaromatic tautomers with CH_2 bridges were 21.46-32.32 kcal/mol higher in energy. **BCC-c-22,23H** is approx. 10-12 kcal/mol less stable due to the presence of a less favorable conjugation pathway that runs through an amine-type nitrogen, and because the two NHs are adjacent to one another. Tautomers **BCC-c-21,22H** and **BCC-c-21,23H** have internal methylene units and π-conjugation can occur through the exterior of ring *a* (18π electron pathway) or through the fused benzo-unit (22π electron pathway). Both forms are much higher in energy but nevertheless are strongly aromatic species. **BCC-c-21,22H** has a NICS(0) value of -8.92 ppm and shows an increased NICS value for the benzo-unit, indicating that the 22π conjugation circuit (structure **30**) is an important contributor. This pathway is also evident in the AICD plot (Figure 15). The

structure of **BCC-c-21,23H** disrupts the 6π electron arene structure and while an 18π electron circuit is still possible in this tautomer, this route (**31a**) appears to be overwhelmed by the 22π electron pathway **31b**. Both of these pathways must pass through an amine-type nitrogen for **BCC-c-21,23H**, so it is remarkable that the global aromatic character (NICS(0) = -11.90 ppm) is substantially larger than is seen for **BCC-c-21,22H**. Nevertheless, the proposed π-circuit is evident in the AICD plot for this species (Figure 15).

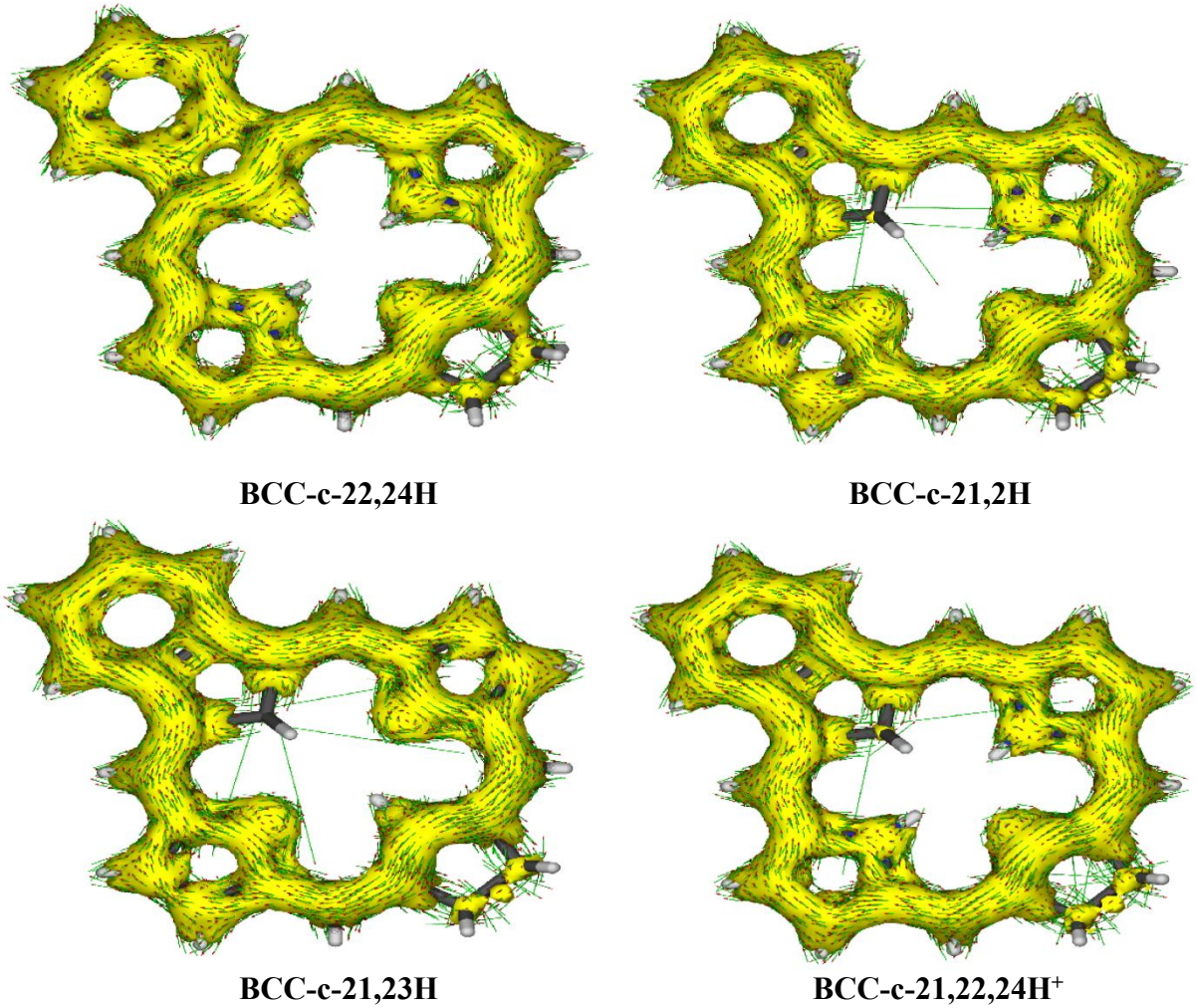

Figure 15. AICD plots (isovalues = 0.05) for benzocarbachlorin tautomers **BCC-c-22,24H**, **BCC-c-21,22H** and **BCC-c-21,23H** and for monocation **BCC-c-21,22,24H**$^+$. **BCC-c-22,24H** shows a porphyrin-like 18π electron delocalization pathway that bypasses the benzo-unit. However, the remaining structures favor 22π electron pathways that run around the benzo-moiety.

Table 4. Calculated Relative Energies (kcal/mol) and NICS Values (ppm) for Benzocarbachlorin Tautomers.

	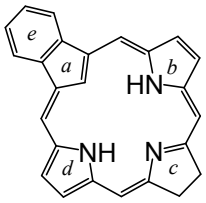	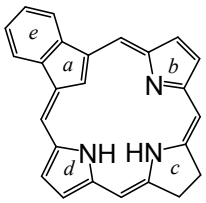	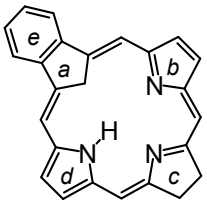	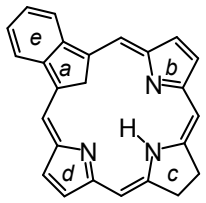
Molecule	**BCC-c-22,24H**	**BCC-c-22,23H**	**BCC-c-21,22H**	**BCC-c-21,23H**
ΔG (298 K)	0.00	+12.15	+15.83	+21.70
ΔE (B3LYP/ **M06-2X**/ B3LYP-D3)	(0.00/ **0.00**/ 0.00)	(+11.62/ **+9.71**/ +11.80)	(+16.73/ **+16.49**/ +16.90)	(+21.79/ **+23.49**/ +21.70)
NICS(0)/NICS(1)$_{zz}$	-11.70/-30.07	-6.48/-15.84	-8.92/-20.93	-11.90/-29.35
NICS(*a*)/NICS(1*a*)$_{zz}$	+2.46/+1.18	+2.79/+3.19	-9.89/-30.30	-13.62/-40.75
NICS(*b*)/NICS(1*b*)$_{zz}$	-13.28/-31.95	-3.57/-15.03	+0.20/-7.88	-2.45/-13.68
NICS(*c*)/NICS(1*c*)$_{zz}$	+6.98/+10.71	+2.64/+7.90	+5.85/+9.54	+6.91/+16.99
NICS(*d*)/NICS(1*d*)$_{zz}$	-13.30/-31.61	-13.70/-28.54	-14.39/-35.05	-2.45/-13.68
NICS(*e*)/NICS(1*e*)$_{zz}$	-6.27/-22.41	-6.51/-22.92	-9.49/-30.60	-8.86/-29.52
	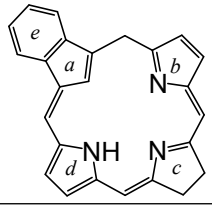	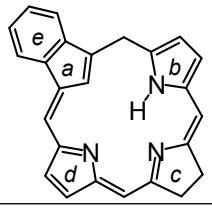	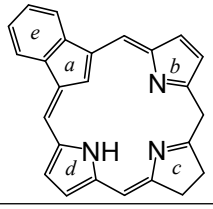	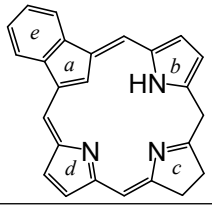
Molecule	**BCC-c-5,24H**	**BCC-c-5,22H**	**BCC-c-10,24H**	**BCC-c-10,22H**
ΔG (298 K)	+25.27	+29.23	+22.87	+25.48
ΔE (B3LYP/ **M06-2X**/ B3LYP-D3)	(+26.97/ **+24.59**/ +27.98)	(+31.36/ **+29.81**/ +32.32)	(+24.98/ **+21.46**/ +26.02)	(+27.65/ **+23.89**/ +28.74)
NICS(0)/NICS(1)$_{zz}$	-0.97/-0.47	-1.25/-1.28	+0.17/+2.40	+0.58/+3.47
NICS(*a*)/NICS(1*a*)$_{zz}$	+2.49/+2.64	+5.65/+9.31	+1.06/-0.50	+1.14/-0.36
NICS(*b*)/NICS(1*b*)$_{zz}$	+0.13/-7.45	-12.11/-26.27	-2.62/-12.18	-11.38/-25.07
NICS(*c*)/NICS(1*c*)$_{zz}$	+2.03/+1.76	+2.12/+2.27	+1.73/+0.64	+1.62/-0.08
NICS(*d*)/NICS(1*d*)$_{zz}$	-10.75/-24.58	-0.15/-7.46	-10.09/-22.69	-1.36/-9.04
NICS(*e*)/NICS(1*e*)$_{zz}$	-6.94/-23.43	-6.22/-21.74	-7.42/-24.43	-7.46/-24.65

Table 5. Calculated Relative Energies (kcal/mol) and NICS Values (ppm) for Tautomers of Benzocarbachlorin Monocations.

	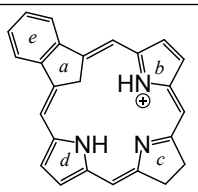	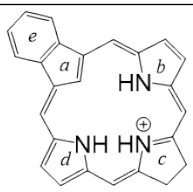	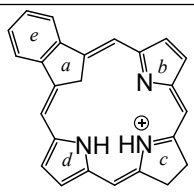	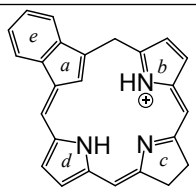	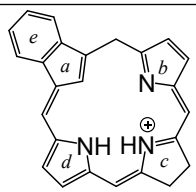
Molecule	**BCC-c-21,22,24H$^+$**	**BCC-c-22,23,24H$^+$**	**BCC-c-21,22,23H$^+$**	**BCC-c-5,22,24H$^+$**	**BCC-c-5,23,24H$^+$**
ΔG (298 K)	0.00	+8.97	+12.61	+15.61	+28.75
ΔE (B3LYP/ **M06-2X**/ B3LYP-D3)	(0.00/ **0.00**/ 0.00)	(+8.27/ **+4.78**/ +8.07)	(+12.82/ **+12.11**/ +12.88)	(+16.74/ **+16.08**/ +17.44)	(+29.76/ **+27.51**/ +30.64)
NICS(0)/NICS(1)$_{zz}$	-13.08/-31.57	-7.91/-18.54	-10.14/-23.83	-3.37/-6.46	-2.76/-5.29
NICS(*a*)/NICS(1*a*)$_{zz}$	-15.48/-44.07	+3.51/+4.30	-11.80/-34.73	+6.41/+10.44	+5.65/+10.09
NICS(*b*)/NICS(1*b*)$_{zz}$	-13.18/-33.69	-12.61/-24.82	+1.21/-5.10	-10.48/-23.24	+1.88/-3.33
NICS(*c*)/NICS(1*c*)$_{zz}$	+8.24/+14.84	+3.71/+6.12	+5.65/+13.51	+3.27/+4,21	+1.81/+5.34
NICS(*d*)/NICS(1*d*)$_{zz}$	-13.18/-33.71	-12.65/-24.85	-14.79/-31.13	-8.37/-19.99	-10.82/-22.27
NICS(*e*)/NICS(1*e*)$_{zz}$	-10.45/-33.60	-6.63/-23.18	-9.10/-30.50	-5.83/-20.19	-6.15/-21.35
	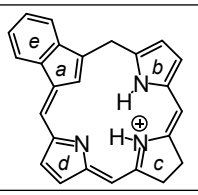	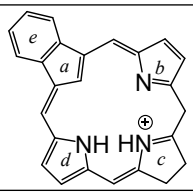	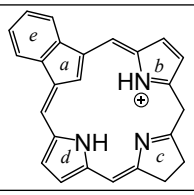	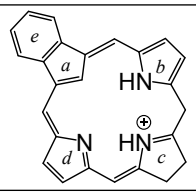	
Molecule	**BCC-c-5,22,23H$^+$**	**BCC-c-10,23,24H$^+$**	**BCC-c-10,22,24H$^+$**	**BCC-c-10,22,23H$^+$**	
ΔG (298 K)	+27.45	+29.72	+11.70	+32.52	
ΔE (B3LYP/ **M06-2X**/ B3LYP-D3)	(+28.29/ **+25.25**/ +29.12)	(+30.53/ **+25.23**/ +31.59)	(+12.54/ **+7.99**/ +13.30)	(+33.76/ **+27.37**/ +34.83)	
NICS(0)/NICS(1)$_{zz}$	-1.30/-0.22	-0.10/+1.60	+0.19/+2.30	+2.76/+10.03	
NICS(*a*)/NICS(1*a*)$_{zz}$	+10.80/+19.78	+2.95/+4.86	+0.41/-0.24	+0.92/-3.65	
NICS(*b*)/NICS(1*b*)$_{zz}$	-12.00/-29.35	-4.01/-14.99	-10.11/-21.82	-10.33/-20.92	
NICS(*c*)/NICS(1*c*)$_{zz}$	+0.29/+4.80	+0.47/+2.34	+1.88/+0.78	-8.64/-4.91	
NICS(*d*)/NICS(1*d*)$_{zz}$	+3.47/-0.17	-10.60/-22.08	-7.50/-17.73	-2.95/-11.17	
NICS(*e*)/NICS(1*e*)$_{zz}$	-4.39/-16.32	-6.97/-23.61	-7.72/-25.43	-7.77/-24.94	

Nine tautomers of monoprotonated **BCC** were analyzed and the most stable form proved to be C-protonated **BCC-c-21,22,24H$^+$** rather than the expect N-protonated structure **BCC-c-22,23,24H$^+$** (Table 5). The more stable tautomer is highly diatropic with a NICS(0) value of -13.08 ppm and rings *a*, *b*, *d* and *e* all gave large negative NICS values. These results were consistent with

the 23-atom 22π electron delocalization pathway shown in structure **32**, an outcome that is also supported by AICD calculations (Figure 15). The C1-C2 and C3-C4 bonds, which connect the benzo-unit to the rest of the macrocycle, are ca. 0.04 Å shorter than in the free base demonstrating increases conjugative connectivity, although more pronounced bond length alternation emerges in the arene unit. The NICS(0) value for **BCC-c-22,23,24H**$^+$, while substantial, is less than -8 ppm indicating reduced aromaticity and the results suggest that a porphyrin-like 18π electron pathway is favored for this species. It was not possible to obtain the proton NMR spectrum for monoprotonated benzocarbachlorin **27a** but the related aldehydes **27b,c** gave conventional N-protonated monocations **27b,c**H$^+$ (Scheme 5) in contradiction to the computational results. In tautomer **BCC-c-22,23,24H**$^+$, the benzo-unit is effectively disconnected from the global conjugation pathways and the presence of an electron-withdrawing formyl moiety would not significantly affect the stability of the monocation. However, the presence of an aldehyde substituent on the benzo-fragment of **BCC-c-21,22,24H**$^+$ would directly interact with the 22π electron delocalization pathway and would thereby destabilize the structure. Hence, the N-protonated tautomer is more favored under these circumstances. The alternative C-protonated monocation **BCC-c-21,22,23H**$^+$ was calculated to be >12 kcal/mol higher in energy, presumably due to unfavorable steric interactions between the adjacent NHs. In addition, the core arrangement in **BCC-c-21,22,24H**$^+$ is set up for much more favorable hydrogen bonding interactions. The remaining tautomers are protonated onto one of the *meso*-carbon bridges and four of the six structures show increases in the relative energies that were close to 30 kcal/mol. However, **BCC-c-22,23,24H**$^+$ and **BCC-c-22,23,24H**$^+$ were far more accessible species (relative energies between 7.99 and 17.44 kcal/mol) because these have macrocyclic cores that are arranged to maximize intramolecular hydrogen bonding interactions. Three dications were also considered (Table 6) but

only the most stable form was aromatic. As these structures only differ by the placement of a single hydrogen atom, they have been designated to show the position of this atom. Two of the tautomers, **BCC-c-5H^{2+}** and **BCC-c-10H^{2+}**, have interrupted conjugation due to the presence of methylene bridges. The favored aromatic tautomer, **BCC-c-21H^{2+}**, gave a NICS(0) value of -11.96 and produced large negative NICS values for rings *a*, *b*, *d* and *e* as well. This indicates that the macrocycle again favors a 23-atom 22π electron pathway as shown in structure **33** (Figure 13). The AICD plot also clearly demonstrates the presence of this conjugation pathway (Figure 16). The presence of an electron-withdrawing formyl unit on the benzo-component would destabilize the dication and this explains why diprotonation of carbachlorins **27b,c** was not favored.

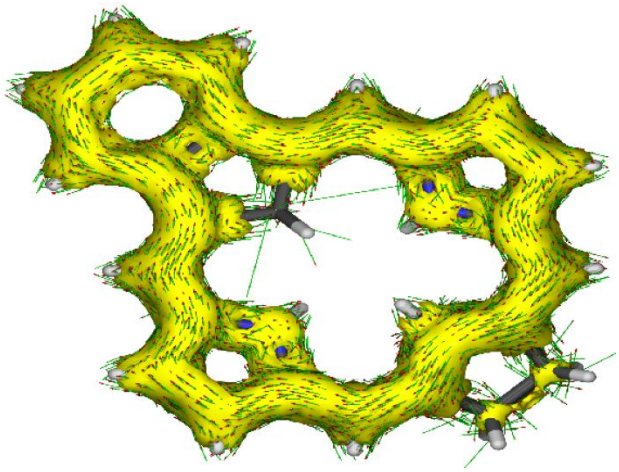

Figure 16. AICD plot (isovalue = 0.05) of benzocarbachlorin dication **BCC-c-21H^{2+}**.

Table 6. Calculated Relative Energies (kcal/mol) and NICS Values (ppm) for Unsubstituted Benzocarbachlorin Dications.

	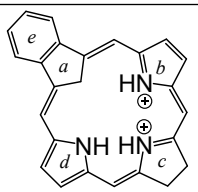	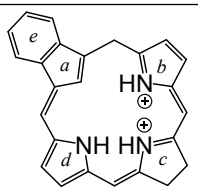	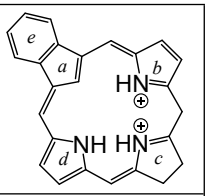
Molecule	**BCC-c-21H^{2+}**	**BCC-c-5H^{2+}**	**BCC-c-10H^{2+}**
ΔG (298 K)	0.00	+17.31	+19.32
ΔE (B3LYP/ **M06-2X**/ B3LYP-D3)	(0.00/ **0.00**/ 0.00)	(+18.38/ **+18.10**/ +19.06)	(+19.69/ **+14.07**/ +20.55)
NICS(0)/NICS(1)$_{zz}$	-11.96/-27.25	-3.59/-6.21	+0.57/+4.78
NICS(*a*)/NICS(1*a*)$_{zz}$	-14.30/-40.12	+15.78/+29.10	+2.06/+3.13
NICS(*b*)/NICS(1*b*)$_{zz}$	-13.22/-23.69	-10.68/-18.99	-9.51/-18.07
NICS(*c*)/NICS(1*c*)$_{zz}$	+7.09/+11.76	+2.08/+4.93	-0.33/+0.13
NICS(*d*)/NICS(1*d*)$_{zz}$	-13.23/-23.71	-5.81/-11.73	-8.15/-17.40
NICS(*e*)/NICS(1*e*)$_{zz}$	-9.58/-33.08	-0.99/-7.63	-7.37/-24.72

Conclusion

Carbachlorins are an important class of porphyrin analogues that have similar electronic properties to tetrapyrrolic chlorins while possessing improved stability towards oxidation. In order to expand our knowledge in this area, new families of carbachlorins have been synthesized. The *tert*-butyl ester protective groups of a dihydrodipyrrin-aldehyde and a pyrrolylmethylazulene-aldehyde were cleaved with TFA, and following dilution with acetic acid and further acidification with HI, cross-condensation produced monoprotonated azulichlorins. Azulichlorin monocations possess macrocyclic aromaticity and their UV-vis spectra give strong Soret bands. The free-base forms of azulichlorins are relatively unstable compared to the protonated species and they slowly oxidize over time to give impure carbachlorins. Proton NMR studies on the mono- and diprotonated forms of azulichlorins indicated that diprotonation reduced the diatropic characteristics. Oxidative ring contraction of an azulichlorin with *tert*-butyl hydroperoxide and KOH gave a novel benzocarbachlorin in 24% yield, together with an isomeric mixture of

benzocarbachlorin-aldehydes in 37-46% yield. These benzocarbachlorins exhibit strongly aromatic characteristics and the proton NMR spectra showed the internal C-H near -4.7 ppm. Protonation of benzocarbachlorin favored the formation of a dicationic species that enhanced diatropic character due in part to the formation of a 22π electron delocalization pathway. On the other hand, addition of acid to benzocarbachlorin-aldehydes primarily resulted in the formation of monocations, indicating that the electron withdrawing aldehyde groups decrease the basicity of the carbachlorin core.

Experimental Section

Melting points are uncorrected. NMR spectra were recorded using a 400 or 500 MHz NMR spectrometer and were run at 302 K unless otherwise indicated. ^{1}H NMR values are reported as chemical shifts δ, relative integral, multiplicity (s, singlet; d, doublet; t, triplet; q, quartet; m, multiplet; br, broad peak) and coupling constant (*J*). Chemical shifts are reported in parts per million (ppm) relative to $CDCl_3$ (^{1}H residual $CHCl_3$ δ 7.26, ^{13}C $CDCl_3$ triplet δ 77.23), and coupling constants were taken directly from the spectra. NMR assignments were made with the aid of ^{1}H-^{1}H COSY, HSQC, DEPT-135, and NOE difference proton NMR spectroscopy. 2D experiments were performed by using standard software. High- resolution mass spectra (HRMS) were carried out by using a double focusing magnetic sector instrument. ^{1}H and ^{13}C NMR spectra for all new compounds are reported in Supporting Information.

***tert*-Butyl *E*-5-(4,4-dimethyl-5-oxo-3,4-dihydro-furan-2-ylidene)-3-ethyl-4-methyl-1*H*-pyrrole-2-carboxylate (17).** A solution of iodopyrrole **15**[52] (4.00 g, 11.9 mmol), alkyne carboxylic acid **16** (2.30 g, 18.2 mmol), benzyltriethylammonium chloride (4.46 g, 14.0 mmol) and triethylamine (29 mL) in acetonitrile (146 mL) was purged with nitrogen for 10 min and then

treated with $Pd(PPh_3)_4$ (1.42 g, 1.1 mmol). The resulting mixture was heated under reflux for 17 h. At the end of this period, the solvent was removed under reduced pressure and the residue partitioned between dichloromethane and water. The organic layer was washed with water, dried over magnesium sulfate, filtered, and evaporated under reduced pressure. The residue was purified by flash chromatography on silica gel eluting with 5% ethyl acetate-hexanes to give lactone **17** (3.45 g, 10.3 mmol, 87%) as a colorless crystalline solid, mp 128-129 °C. ^{1}H NMR (500 MHz, $CDCl_3$): δ 1.06 (3H, t, J = 7.6 Hz, CH_2CH_3), 1.35 (6H, s, *gem*-diMe), 1.58 (9H, s, *t*-Bu), 2.24 (3H, s, pyrrole-CH_3), 2.42 (2H, q, J = 7.6 Hz, CH_2CH_3), 2.97 (2H, d, J = 2.1 Hz, lactone-CH_2), 6.21 (1H, t, J = 2.1 Hz, bridge-CH), 8.33 (1H, br s, NH). $^{13}C\{^1H\}$ NMR (125 MHz, $CDCl_3$): δ 10.5 (pyrrole-Me), 15.7 (CH_2CH_3), 17.5 (CH_2CH_3), 25.4 (*gem*-diMe), 28.7 (*t*-Bu), 40.3 (CMe_2), 40.6 (lactone-CH_2), 81.0 ($OCMe_3$), 97.1 (bridge-CH), 120.8, 125.7, 125.9, 127.4, 147.5, 161.8 (ester-C=O), 179.2 (lactone-C=O). EI MS: *m/z* (rel. int.) 333 (23, M^+), 277 (100, $[M - C_4H_8]^+$), 262 (10, $[M - C_4H_8 - CH_3]^+$), 260 (10, $[M - C_4H_9O]^+$), 233 (9, $[M - C_4H_8 - CO_2]^+$), 193 (86). HRMS (EI): *m/z* Calcd for $C_{19}H_{27}NO_4$ 333.1940, found 333.1946.

***tert*-Butyl *E*-5-(4,4-dimethyl-5-methylene-3,4-dihydro-furan-2-ylidene)-4-ethyl-3-methyl-1*H*-pyrrole-2-carboxylate (18).** A suspension of titanocene dichloride (1.47 g; 5.97 mmol) in anhydrous toluene (16 mL) was treated with 8.2 mL (13.1 mmol) of 1.6 M methyllithium in diethyl ether over 5 min at 0 °C. After stirring the solution for 1 h at 0 °C, the reaction was quenched with 14 mL of 6% aqueous ammonium chloride solution. The organic layer was separated and washed sequentially with water and brine, dried over sodium sulfate, and filtered to give an orange solution of dimethyl titanocene. Lactone **17** (0.420 g, 1.26 mmol) and titanocene dichloride (19 mg; 0.076 mmol) were added to the solution, and the mixture was refluxed for 24 h. The flask was cooled to

room temperature and methanol (1.5 mL), sodium bicarbonate (63 mg) and water (15 μL) were added. The resulting solution was stirred for 12 h at 40 °C, filtered through a pad of Celite and the residue further washed with hexanes. If necessary, the filtrate was filtered a second time, and the solvents were then removed under reduced pressure. The resulting oil was purified by flash chromatography on silica gel eluting with 20% dichloromethane-hexanes containing 1% triethylamine. Following evaporation of the solvents, the enol ether (0.32 g, 0.96 mmol, 76%) was obtained as yellow crystals, mp 86-90 °C. ^{1}H NMR (500 MHz, $CDCl_3$): δ 1.05 (3H, t, J = 7.5 Hz, CH_2CH_3), 1.27 (6H, s, *gem*-diMe), 1.57 (9H, s, *t*-Bu), 2.27 (3H, s, pyrrole-CH_3), 2.44 (2H, q, J = 7.5 Hz, CH_2CH_3), 2.72 (2H, d, J = 1.9 Hz, CH_2CMe_2), 4.02 (1H, d, J = 2.4 Hz), 4.40 (1H, d, J = 2.4 Hz) (=CH_2), 5.95 (1H, t, J = 1.9 Hz, bridge-CH), 8.30 (1H, br s. NH). $^{13}C\{^1H\}$ NMR (125 MHz, $CDCl_3$): δ 10.6 (pyrrole-Me), 15.7 (CH_2CH_3), 17.5 (CH_2CH_3), 28.0 (*gem*-diMe), 28.8 (*t*-Bu), 40.6 (CMe_2), 42.5 (CH_2CMe_2), 80.6 ($OCMe_3$), 81.0 (=CH_2), 92.0 (bridge-CH), 119.6, 125.7, 125.8, 128.1, 153.8, 161.8, 169.1. EI MS: *m/z* (rel. int.) 331 (22, M^+), 275 (100, $[M - C_4H_8]^+$), 260 (24, $[M - C_4H_8 - CH_3]^+$), 242 (23). HRMS (EI): *m/z* Calcd for $C_{20}H_{29}NO_3$ 331.2147, found 331.2151.

***tert*-Butyl *Z*-4-ethyl-3-methyl-5-(4,4,5-trimethyl-3,4-dihydropyrrol-2-ylidene)-1*H*-pyrrole-2-carboxylate** (**14**). A solution of enol ether **18** (1.02 g, 3.08 mmol) in DMF (24 mL) was treated with 210 μL (0.13 mmol) of 6 M HCl and stirred at room temperature until the formation of diketone **19** was complete (ca. 1 h; monitored by TLC, R_f on silica with 20% ethyl acetate-hexanes of 0.20). The reaction was then treated with ammonium acetate (8.0 g, 10.2 mmol) and triethylamine (14 mL, 10.2 mmol) and the resulting solution heated at 55 °C until product formation was complete by TLC (ca. 6 h; R_f on silica with 20% ethyl acetate-hexanes of 0.55).

The mixture was diluted with 10% KH_2PO_4 (24 mL) and extracted with dichloromethane (3 × 25 mL). The combined organic extracts were washed sequentially with water (2 × 50 mL) and brine, dried over sodium sulfate, filtered, and concentrated under reduced pressure. The resulting oil was purified by flash chromatography on silica gel eluting with 10% ethyl acetate-hexanes to give the dihydrodipyrrin (0.71 g, 2.15 mmol, 70%) as a red crystalline solid, mp 118-120°C. ^{1}H NMR (500 MHz, $CDCl_3$): δ 1.07 (3H, t, J = 7.5 Hz, CH_2CH_3), 1.18 (6H, s, *gem*-diMe), 1.57 (9H, s, *t*-Bu), 2.14 (3H, s, imine-CH_3), 2.27 (3H, s, pyrrole-CH_3), 2.44 (2H, q, J = 7.5 Hz, CH_2CH_3), 2.58 (2H, d, J = 1.8 Hz, pyrroline-CH_2), 5.82 (1H, br t, bridge-CH), 11.08 (1H, br s, NH). $^{13}C\{^1H\}$ NMR (125 MHz, $CDCl_3$): δ 10.3 (pyrrole-Me), 15.9 (imine-Me), 16.3 (CH_2CH_3), 17.3 (CH_2CH_3), 25.8 (*gem*-diMe), 28.7 (*t*-Bu), 44.7 (pyrroline-CH_2), 48.5 (CMe_2), 79.7 ($OCMe_3$), 103.4 (bridge-CH), 119.8, 125.2, 125.5, 130.1, 151.5, 161.3, 188.0. EI MS: *m/z* (rel. int.) 330 (28, M^+), 274 (100, [M - C_4H_8]$^+$), 259 (18, [M - C_4H_8 - CH_3]$^+$), 241 (26). HRMS (EI): *m/z* Calcd for $C_{20}H_{30}N_2O_2$ 330.2307, found 330.2310.

***tert*-Butyl *Z*-5-(5-formyl-3,4-dihydro-4,4-dimethylpyrrol-2-ylidene)-4-ethyl-3-methyl-1*H*-pyrrole-2-carboxylate (20)**. Selenium dioxide (289 mg, 2.60 mmol) was added to a solution of dihydrodipyrrin **14** (717 mg, 2.17 mmol) in DMF (20 mL) and pyridine (210 μL, 2.60 mmol) and stirred at room temperature for 5 h. The mixture was then heated to 80°C for 15 min, cooled to room temperature, filtered, and poured into water. The mixture was extracted with dichloromethane (3 × 10 mL), and the combined organic extracts were washed sequentially with saturated aqueous sodium bicarbonate and brine, dried over Na_2SO_4, filtered, and the solvent removed under reduced pressure. The resulting oil was purified by flash chromatography on silica gel eluting with toluene to give the aldehyde (346 mg, 1.00 mmol, 46%) as an orange crystalline

solid, mp 119-121 °C. ^{1}H NMR (500 MHz, $CDCl_3$): δ 1.10 (3H, t, J = 7.6 Hz, CH_2CH_3), 1.36 (6H, s, *gem*-diMe), 1.58 (9H, s, *t*-Bu), 2.28 (3H, s, pyrrole-CH_3), 2.50 (2H, q, J = 7.6 Hz, CH_2CH_3), 2.74 (2H, d, J = 1.8 Hz, pyrroline-CH_2), 6.24 (1H, t, J = 1.8 Hz, bridge-CH), 9.92 (1H, s, CHO), 10.78 (1H, br s, NH). $^{13}C\{^1H\}$ NMR (125 MHz, $CDCl_3$): δ 10.2 (pyrrole-Me), 16.4 (CH_2CH_3), 17.4 (CH_2CH_3), 25.8 (*gem*-diMe), 28.7 (*t*-Bu), 46.5 (CMe_2), 46.6 (pyrroline-CH_2), 80.6 ($OCMe_3$), 113.1 (bridge-CH), 122.9, 125.6, 129.1, 129.4, 150.9, 160.9, 177.8, 190.3 (CHO). EI MS: *m/z* (rel. int.) 344 (25, M^+), 288 (27, $[M - C_4H_8]^+$), 273 (100, $[M - C_4H_8 - CH_3]^+$), 255 (45), 241 (14). HRMS (EI): *m/z* Calcd for $C_{20}H_{28}N_2O_3$ 344.2100, found 344.2096.

***tert*-Butyl 5-(6-*tert*-butyl-1-azulenylmethyl)-4-ethyl-3-methylpyrrole-2-carboxylate (23b)**. *tert*-Butylazulene (489 mg, 2.66 mmol) and *tert*-butyl 5-acetoxymethyl-4-ethyl-3-methylpyrrole-2-carboxylate[53] (**22**, 740 mg, 2.63 mmol) were dissolved in 2-propanol (40 mL) and acetic acid (4 mL), and the solution was refluxed with stirring under nitrogen for 16 h. The solvent was evaporated under reduced pressure and the residue purified by column chromatography on silica eluting initially with 40% dichloromethane−hexanes and then with gradually increased proportions of CH_2Cl_2. Initially a blue fraction corresponding to unreacted 6-*tert*-butylazulene was collected, followed by a major blue band for the title compound. A third blue band corresponding to an azulitripyrrane byproduct was also collected. Following evaporation of the solvent, the azulidipyrrane (680 mg, 1.68 mmol, 63%) was obtained as a dark blue solid, mp 124-126 °C. A sample was recrystallized from ethanol-water to give dark blue crystals, mp 125-126 °C. ^{1}H NMR (500 MHz, $CDCl_3$) δ 1.13 (3H, t, J = 7.5 Hz, CH_2CH_3), 1.45 (9H, s), 1.48 (9H, s) (2 x *t*-Bu), 2.28 (3H, s, pyrrole-CH_3), 2.53 (2H, q, J = 7.5 Hz, CH_2CH_3), 4.34 (2H, s, bridge-CH_2), 7.25 (1H, d, J = 3.8 Hz, 2-H), 7.29-7.31 (1H, m), 7.31-7.33 (1H, m) (5,7-H), 7.62 (1H, d, J = 3.8 Hz), 8.13 (1H,

br s, NH), 8.18 (1H, d, J = 10.6 Hz), 8.24 (1H, d, J = 10.5 Hz) (4,8-H). $^{13}C\{^1H\}$ NMR ($CDCl_3$) δ 10.7 (pyrrole-Me), 15.7 (CH_2CH_3), 17.6 (CH_2CH_3), 24.4 (bridge-CH_2), 28.7 (ester *t*-Bu), 32.1 (azulene-t-Bu), 38.8 (6-CMe_3), 80.1 ($OCMe_3$), 116.7 (2-CH), 118.6, 120.6 (5- or 7-CH), 121.0 (5- or 7-CH), 123.3, 125.0, 126.0, 132.1, 132.6 (4- or 8-CH), 135.1, 136.1 (4- or 8-CH), 137.0 (3-CH), 139.9, 161.5, 161.8. HRMS (EI) calcd for $C_{27}H_{35}NO_2$ 405.2668, found 405.2661.

3(5-*tert*-Butoxycarbonyl-3-ethyl-4-methyl-2-pyrrolylmethyl)-azulene-1-carbaldehyde (**21a**). Phosphorus oxychloride (0.6 mL) was added dropwise to DMF (1 mL) in a 250 mL round-bottom flask while the temperature was maintained between 10 and 20 °C with the aid of an ice bath. The mixture was allowed to stand for 15 min at room temperature. The Vilsmeier reagent was diluted with 32 mL of CH_2Cl_2, followed by the addition of 4.0 g of potassium carbonate. Azulidipyrrane **23a**[40] (600 mg; 1.72 mmol) in dichloromethane (40 mL) was added dropwise over 10 min. The resulting mixture was stirred at room temperature for 1 hour, and then a solution of sodium acetate trihydrate (22.0 g) in water (40 mL) was added. The resulting biphasic mixture was stirred under reflux for 15 min. The mixture was cooled, the organic layer separated, and the aqueous phase extracted with chloroform. The combined organic layers were dried over sodium sulfate, and evaporated under reduced pressure. The residue was recrystallized from ethanol to give pyrrolylmethylazulene-aldehyde **21a** (450 mg, 1.19 mmol, 69%) as a dark-purple powder, mp 147-149 °C. ^1H NMR (500 MHz, $CDCl_3$): δ 1.08 (3H, t, J = 7.5 Hz, CH_2CH_3), 1.50 (9H, s, *t*-Bu), 2.28 (3H, s, pyrrole-Me), 2.49 (2H, q, J = 7.5 Hz, CH_2CH_3), 4.32 (2H, s, bridge-CH_2), 7.51 (1H, t, J = 9.8 Hz, 7-H), 7.62 (1H, t, J = 9.8 Hz, 5-H), 7.86 (1H, t, J = 9.9 Hz, 6-H), 8.03 (1H, s, 2-H), 8.26 (1H, br s, NH), 8.41 (1H, d, J = 9.8 Hz, 8-H), 9.56 (1H, d, J = 9.7 Hz, 4-H), 10.31 (1H, s, CHO). $^{13}C\{^1H\}$ NMR (125 MHz, $CDCl_3$): δ 10.7 (pyrrole-Me), 15.7 (CH_2CH_3), 17.6 (CH_2CH_3), 24.4

(bridge-CH_2), 28.7 (*t*-Bu), 80.5 (O*C*Me_3), 119.2, 124.0, 124.8, 126.0, 127.4, 128.0 (7-CH), 129.9 (5-CH), 130.2, 136.0 (8-CH), 137.8 (4-CH), 140.3 (6-CH), 141.5, 142.3 (2-CH), 142.5, 161.6 (ester C=O), 186.4 (CHO). EI MS: *m/z* (rel. int.) 377 (20, M^+), 354 (26), 321 (14, [M - C_4H_8]$^+$), 308 (19), 277 (32), 274 (45), 273 (35), 255 (16). HRMS (EI): *m/z* Calcd for $C_{24}H_{27}NO_3$ 377.1991, found 377.1994.

6-*tert*-Butyl-3(5-*tert*-butoxycarbonyl-3-ethyl-4-methyl-2-pyrrolylmethyl)-azulene-1-carbaldehyde (**21b**)**.** Phosphorus oxychloride (0.3 mL) was added dropwise to DMF (0.5 mL) in a 100 mL round-bottom flask while the temperature was maintained between 10 and 20 °C with the aid of an ice bath. The mixture was allowed to stand for 15 min at room temperature. The Vilsmeier reagent was diluted with 16 mL of CH_2Cl_2, followed by the addition of 2.0 g of potassium carbonate. Pyrrolylmethylazulene **23b** (300 mg, 0.74 mmol) in dichloromethane (20 mL) was added dropwise over 10 min. The resulting mixture was stirred at room temperature for 1 hour, and then a solution of sodium acetate trihydrate (11.0 g) in water (20 mL) was added. The resulting biphasic mixture was stirred under reflux for 15 min. The mixture was cooled, the organic layer separated, and the aqueous phase extracted with chloroform. The combined organic layers were dried over sodium sulfate, and evaporated under reduced pressure. The residue was recrystallized from ethanol to give the azulidipyrrin-aldehyde **21b** (220 mg, 0.51 mmol, 68%), as a dark-maroon powder, mp 198-200 °C. ^{1}H NMR (500 MHz, $CDCl_3$): δ 1.09 (3H, t, *J* = 7.5 Hz, CH_2CH_3), 1.48 (9H, s), 1.49 (9H, s) (2 x *t*-Bu), 2.28 (3H, s, pyrrole-CH_3), 2.50 (2H, q, *J* = 7.5 Hz, CH_2CH_3), 4.29 (2H, s, bridge-CH_2), 7.69 (1H, dd, *J* = 1.9, 10.6 Hz, 7-H), 7.80 (1H, dd, *J* = 1.8, 10.6 Hz, 5-H), 7.96 (1H, s, 2-H), 8.21 (1H, br s, NH), 8.33 (1H, d, *J* = 10.6 Hz, 8-H), 9.47 (1H, d, *J* = 10.6 Hz, 4-H), 10.28 (1H, s, CHO). ^{13}C{^{1}H} NMR (125 MHz, $CDCl_3$): δ 10.7 (pyrrole-Me),

15.8 (CH_2CH_3), 17.6 (CH_2CH_3), 24.3 (bridge-CH_2), 28.7 (ester *t*-Bu), 32.0 (azulene *t*-Bu), 39.2 (azulene-CMe_3), 80.4 ($OCMe_3$), 119.1, 123.8, 124.6, 126.0, 126.64 (7-CH), 126.68, 127.9 (5-CH), 130.6, 135.0 (8-CH), 136.9 (4-CH), 140.4, 141.2 (2-CH), 141.4, 161.6, 165.1, 186.2 (CHO). EI MS: *m/z* (rel. int.) 433 (28, M^+), 377 (19, $[M - C_4H_8]^+$), 348 (12, $[M - C_4H_8 - CHO]^+$), 333 (9, $[M - C_4H_8 - CO_2]^+$), 304 (5, $[M - C_4H_8 - CO_2 - CHO]^+$), 213 (61), 165 (100). HRMS (EI): *m/z* Calcd for $C_{28}H_{35}NO_3$ 433.2617; found 433.2622.

8,17-Diethyl-8,12,12,12,18-tetramethyl-12,13-dihydroazuliporphyrin hydoiodide (**25a.HI**). Azulidipyrrane-aldehyde **21a** (40 mg, 0.106 mmol) and dihydrodipyrrin-aldehyde **20** (36.5 mg, 0.106 mmol) were dissolved in 5 mL of TFA and stirred at room temperature for 10 min in the dark. The solution was diluted with 100 mL of acetic acid, 14 drops of hydroiodic acid were added, and the mixture stirred overnight in the dark. The solution was diluted with CH_2Cl_2 and washed with water. The organic layer was separated, dried with sodium sulfate and evaporated under reduced pressure. The residue was purified on a silica column, eluting with CH_2Cl_2 containing 2-5% methanol. The product, which was collected as a deep green band, was further purified on a grade 3 basic alumina column, eluting with 4% methanol-dichloromethane. The green band was collected, the solvent removed on a rotary evaporator, and the residue dried *in vacuo* to give the azulichlorin (11 mg, 0.018 mmol, 17%) as a dark-green powder, mp >300 °C. UV-Vis (1% Et_3N-$CHCl_3$): λ_{max}/nm (log ε) 348 (4.55), 391 (sh, 4.55), 410 (sh, 4.59), 439 (4.64), 483 (sh, 4.64). UV-Vis ($CHCl_3$): λ_{max}/nm ($\log_{10}$ ε) 368 (4.57), 408 (sh, 4.62), 418 (sh, 4.65), 444 (4.92), 497 (sh, 4.22), 615 (4.30), 657 (4.27). UV-vis (5% TFA-$CHCl_3$): λ_{max}/nm (log ε) 345 (4.57), 457 (5.00), 505 (4.37), 605 (sh, 4.30), 645 (4.41). ^{1}H NMR (500 MHz, $CDCl_3$): δ -2.11 (1H, s, 21-H), -0.41 (1H,

br s), -0.28 (1H, br s) (2 x NH), 1.53 (3H, t, J = 7.8 Hz, 7-CH_2CH_3), 1.60 (3H, t, J = 7.7 Hz, 17-CH_2CH_3), 1.71 (6H, s, *gem*-diMe), 2.98 (3H, s, 8-CH_3), 3.23 (3H, s, 18-CH_3), 3.34 (2H, q, J = 7.7 Hz, 17-CH_2), 3.79 (2H, q, J = 7.8 Hz, 7-CH_2), 3.82 (2H, s, 13-CH_2), 7.51 (1H, s, 10-H), 7.58 (1H, s, 15-H), 8.06 (1H, t, J = 9.6 Hz, 2^3-H), 8.23 (1H, t, J = 9.6 Hz, 3^2-H), 8.26 (1H, t, J = 9.6 Hz, 2^2-H), 9.22 (1H, s, 20-H), 9.28 (1H, s, 5-H), 10.08 (1H, d, J = 9.6 Hz, 3^1-H), 10.14 (1H, d, J = 9.7 Hz, 2^1-H). $^{13}C\{^1H\}$ NMR (125 MHz, $CDCl_3$): δ 10.5 (8-Me), 11.7 (18-Me), 16.2 (7- CH_2CH_3), 16.9 (17- CH_2CH_3), 18.7 (7-CH_2), 19.6 (17-CH_2), 30.5 (*gem*-diMe), 46.4 (CMe_2), 52.0 (13-CH_2), 90.3 (10-CH), 92.5 (15-CH), 105.2 (5- or 20-CH), 105.4 (5- or 20-CH), 116.9 (21-CH), 125.1, 125.2, 129.7, 135.7, 136.3, 136.44, 136.49, 136.8, 140.0 (3^1-CH), 140.4 (2^1-CH), 140.9, 144.2 (2^3-CH), 146.3, 146.4, 147.3, 147.4, 148.9, 171.3, 182.9. ^1H NMR (500 MHz, TFA-$CDCl_3$, dication **25**H_2^{2+}): δ 1.26 (1H, s, NH), 1.43 (3H, t, J = 7.7 Hz, 17-CH_2CH_3), 1.51 (3H, t, J = 7.7 Hz, 7-CH_2CH_3), 1.82 (6H, s, *gem*-diMe), 2.24 (1H, s, 21-H), 2.79 (3H, s, 8-CH_3), 2.99 (3H, s, 18-CH_3), 3.19 (2H, q, J = 7.7 Hz, 17-CH_2), 3.43 (2H, q, J = 7.7 Hz, 7-CH_2), 3.98 (2H, s, 13-CH_2), 5.40 (1H, br s), 5.41 (1H, br s) (2 x NH), 7.34 (1H, s, 10-H), 7.48 (1H, s, 15-H), 8.19-8.30 (3H, m, 2^2,2^3,3^2-H), 9.238 (1H, s), 9.241 (1H, s) (5,20-H), 9.42 (1H, d, J = 9.4 Hz), 9.43 (1H, d, J = 9.5 Hz) (2^1,3^1-H). $^{13}C\{^1H\}$ NMR (125 MHz, TFA-$CDCl_3$, dication **25**H_2^{2+}): δ 10.4, 11.1, 15.1, 15.9, 18.6, 19.5, 29.5, 44.9, 47.6, 89.1, 91.0, 114.19, 114.22, 126.2, 126.3, 131.4, 132.2, 137.6, 137.7, 138.57, 138.62, 139.0, 139.4, 140.6, 144.2, 145.5, 149.74, 149.77, 150.5, 154.1, 155.2, 155.3, 165.9. HRMS (ESI): *m/z* $[M + H]^+$ Calcd for $C_{34}H_{36}N_3$ 486.2909; found 486.2911.

2^3-*tert*-Butyl-8,17-diethyl-8,12,12,12,18-tetramethyl-12,13-dihydroazuliporphyrin hydoiodide (25b.HI). *tert*-Butylazulidipyrrane-aldehyde **21b** (42 mg, 0.096 mmol) and **20** (36 mg, 0.10 mmol) were reacted under the foregoing conditions. The crude product was purified on

silica column, eluting with 2-5% methanol-dichloromethane, and then on a grade 3 basic alumina column, eluting with 4% methanol-dichloromethane. The resulting major green band was evaporated under reduced pressure and the residue dried overnight in a vacuum desiccator to give the *tert*-butyl azulichlorin (10 mg, 0.015 mmol, 15%) as a dark-green powder, mp >300 °C. UV-Vis (1% Et_3N-$CHCl_3$): λ_{max}/nm (log ε) 348 (4.50), 368 (4.50), 444 (4.59), 595 (sh, 4.07). UV-Vis ($CHCl_3$): λ_{max}/nm (log ε) 366 (4.54), 407 (sh, 4.51), 418 (sh, 4.57), 445 (4.87), 498 (4.22), 615 (4.29), 657 (4.27). UV-vis (5% TFA-$CHCl_3$): λ_{max}/nm (log ε) 341 (4.55), 459 (4.95), 507 (sh, 4.32), 602 (sh, 4.29), 643 (4.44). ^{1}H NMR (500 MHz, $CDCl_3$): δ -1.46 (1H, s, 21-H), 0.13 (1H, br s), 0.21 (1H, br s) (2 x NH), 1.54 (3H, t, *J* = 7.7 Hz, CH_2CH_3), 1.63 (9H, s, *t*-Bu), 1.65 (3H, t, *J* = 7.7 Hz, CH_2CH_3), 1.80 (6H, s, *gem*-diMe), 3.02 (3H, s, 8-CH_3), 3.30 (3H, s, 18-CH_3), 3.39 (2H, q, *J* = 7.7 Hz), 3.81 (2H, q, *J* = 7.7 Hz) (2 x CH_2CH_3), 4.04 (2H, s, 13-CH_2), 7.72 (1H, s, 10-H), 7.83 (1H, s, 15-H), 8.54 (1H, dd, *J* = 1.7, 10.5 Hz), 8.58 (1H, dd, *J* = 1.7, 10.5 Hz) (2^2,3^2-H), 9.60 (1H, s), 9.65 (1H, s) (5,20-H), 10.16 (1H, d, *J* = 10.5 Hz), 10.30 (1H, d, *J* = 10.6 Hz) (2^1,3^1-H). ^{13}C{^{1}H} NMR (125 MHz, $CDCl_3$): δ 10.6, 11.9, 16.2, 17.0, 18.7, 19.7, 30.6, 32.0, 40.2, 46.6, 52.2, 90.5, 92.7, 105.3, 105.6, 116.8, 125.5, 125.8, 129.8, 134.8, 135.1, 135.7, 136.6, 137.0, 139.1, 139.6, 140.7, 146.0, 146.1, 147.13, 147.15, 148.7, 170.3, 171.2, 182.7. ^{1}H NMR (500 MHz, TFA-$CDCl_3$, dication **25b**H_2^{2+}): δ 1.26 (1H, s), 1.44 (3H, t, *J* = 7.6 Hz), 1.52 (3H, t, *J* = 7.7 Hz), 1.63 (9H, s), 1.83 (6H, s), 1.85 (1H, br s), 2.80 (3H, s), 3.00 (3H, s), 3.21 (2H, q, *J* = 7.6 Hz), 3.45 (2H, q, *J* = 7.7 Hz), 4.01 (2H, s), 5.11 (1H, br s), 5.12 (1H, br s), 7.40 (1H, s), 7.54 (1H, s), 8.43 (2H, d, *J* = 10.5 Hz), 9.29 (2H, s), 9.39-9.42 (2H, m). HRMS (ESI): *m/z* $[M + H]^+$ Calcd for $C_{38}H_{44}N_3$ 542.3535; found 542.3536.

8,17-Diethyl-8,12,12,12,18-tetramethyl-12,13-dihydrobenzo[*b*]carbaporphyrin (27a). Potassium hydroxide (100 mg) in 12 mL of methanol and a solution of *tert*-butyl hydroperoxide in decane (5M, 20 μL) were added to a solution of azulichlorin **25a.HI** (10.0 mg, 0.016 mmol) in dichloromethane (12 mL), and the resulting mixture was stirred under nitrogen in the dark for 40 min. The solution was diluted with chloroform, washed with water (2x), dried over sodium sulfate, and evaporated under reduced pressure. The residues were chromatographed on a grade 3 alumina column, eluting initially with 30% dichloromethane-hexanes. An orange band was collected, the solvent evaporated, and the residue recrystallized from chloroform-hexanes to give a yellow-brown powder (1.9 mg, 0.0040 mmol, 24%) corresponding to benzocarbachlorin **27a**, mp >300°C. UV-Vis (1% Et_3N-$CHCl_3$): λ_{max}/nm (log ε) 344 (4.18), 363 (4.18), 414 (4.64), 430 (4.64), 507 (3.81), 515 (3.82), 540 (sh, 3.50), 622 (3.30), 653 (sh, 3.38), 684 (4.29). UV-vis (5% TFA-$CHCl_3$; dication **27a**H_2^{2+}): λ_{max}/nm (log ε) 343 (sh, 4.09), 361 (4.35), 404 (4.80), 484 (sh, 3.71), 557 (3.46), 606 (3.27), 762 (sh, 3.69), 800 (4.44). ^{1}H NMR (500 MHz, $CDCl_3$): δ -4.64 (1H, s, 21-H), -2.63 (1H, br s), -2.58 (1H, br s) (2 x NH), 1.71 (3H, t, J = 7.7 Hz, 17- CH_2CH_3), 1.76 (3H, t, J = 7.7 Hz, 7- CH_2CH_3), 2.01 (6H, s, *gem*-diMe), 3.34 (3H, s, 8-CH_3), 3.44 (3H, s, 18-CH_3), 3.76 (2H, q, J = 7.7 Hz, 17-CH_2), 3.92 (2H, q, J = 7.7 Hz, 7-CH_2), 4.51 (2H, br s, 13-CH_2), 7.65-7.68 (2H, m, 2^2,3^2-H), 8.47 (1H, s, 10-H), 8.59 (1H, s, 15-H), 8.68-8.73 (2H, m, 2^1,3^1-H), 9.72 (1H, s, 20-H), 9.76 (1H, s, 5-H). $^{13}C\{^1H\}$ NMR (125 MHz, $CDCl_3$): δ 10.9 (8-Me), 11.4 (18-Me), 17.1 (17- CH_2CH_3), 17.4 (7- CH_2CH_3), 19.2 (17-CH_2), 19.8 (7-CH_2), 31.5 (*gem*-diMe), 46.4 (CMe_2), 52.7 (13-CH_2), 90.2 (10-CH), 92.1 (15-CH), 101.3 (20-CH), 101.6 (5-CH), 111.4 (21-CH), 120.0 (2^1- & 3^1-CH), 125.43, 125.48 (2^2,3^2-CH), 129.8, 129.9, 130.0, 131.7, 132.9, 133.0, 133.4, 137.6, 138.8, 139.8,

140.37, 140.42, 161.5, 173.1. ^{1}H NMR (500 MHz, TFA-$CDCl_3$, dication **27a**H_2^{2+}): δ -6.77 (2H, s, 21-CH_2), -3.45 (1H, br s), -3.42 (1H, br s) (2 x NH), 1.83 (3H, t, *J* = 7.7 Hz), 1.90 (3H, t, *J* = 7.7 Hz) (2 x CH_2CH_3), 2.18 (6H, s, gem-diMe), 3.60 (3H, s, 8-CH_3), 3.71 (3H, s, 18-CH_3), 4.02 (2H, q, *J* = 7.7 Hz, 17-CH_2), 4.18 (2H, q, *J* = 7.7 Hz, 7-CH_2), 4.88 (2H, s, 13-CH_2), 8.74-8.78 (2H, m, 2^2,3^2-H), 9.47 (1H, s, 10-H), 9.64 (1H, s, 15-H), 10.09-10.12 (2H, m, 2^1,3^1-H), 11.120 (1H, s), 11.126 (1H, s) (5,20-H). ^{13}C{^{1}H} NMR (125 MHz, TFA-$CDCl_3$, dication **27a**H_2^{2+}): δ 11.4 (8-Me), 11.7 (18-Me), 17.2 (CH_2CH_3), 17.3 (CH_2CH_3), 19.7 (17-CH_2), 20.0 (7-CH_2), 31.7 (*gem*-diMe), 32.0 (21-CH_2), 47.8 (12-C), 53.1 (13-CH_2), 101.2 (10-CH), 103.2 (15-CH), 105.8 (5- & 20-CH), 123.64, 123.70 (2^1,3^1-CH), 131.7, 131.8 (2^2,3^2-CH), 134.8, 136.1, 137.8, 138.2, 139.1, 139.6, 136.7, 142.0, 142.9, 143.6, 143.8, 166.6, 178.0. HRMS (ESI): *m/z* $[M + H]^+$ Calcd for $C_{33}H_{36}N_3$ 474.2909; found 474.2908.

Benzocarbachlorin carbaldehydes 27b and **27c.** A second major band was collected (3.0-3.8 mg, 0.0060-0.0076 mmol, 37-46%) corresponding to a 50/50 mixture of benzocarbachlorin-aldehydes, mp >300 °C. UV-Vis (1% Et_3N-$CHCl_3$): λ_{max}/nm (log ε) 342 (4.51), 442 (5.02), 530 (sh, 3.91), 557 (4.10), 616 (3.66), 646 (3.45), 676 (4.45). UV-vis (0.5% TFA-$CHCl_3$; monocations **27b,c**H^+): λ_{max}/nm (log ε) 339 (4.38), 450 (4.93), 535 (3.89), 575 (sh, 3.49), 645 (sh, 3.53), 677 (sh, 3.89), 707 (4.59). ^{1}H NMR (500 MHz, $CDCl_3$): δ -4.70 (s), -4.69 (s) (1H), -2.74 (1H, br s), -2.69 (s), -2.67 (br s) (1H), 1.67-1.74 (6H, m), 2.02 (6H, s), 3.29 (s), 3.30 (s) (3H), 3.34 (3H, s), 3.67-3.72 (2H, m), 3.82 (2H, q, *J* = 7.5 Hz), 4.48 (2H, s), 7.97-8.01 (1H, m), 8.43 (1H, s), 8.52 (1H, s), 8.53-8.58 (1H, m), 8.97 (s), 8.99 (s) (1H), 9.46 (s), 9.51 (s), 9.52 (s), 9.55 (s) (2H), 10.28 (1H, s). ^{13}C{^{1}H} NMR (125 MHz, $CDCl_3$): δ 10.84, 10.86, 11.3, 17.0, 17.36, 17.41, 19.2, 19.69, 19.73,

31.5, 46.5, 52.7, 90.27, 90.31, 92.20, 92.24, 101.5, 101.6, 101.8, 102.0, 112.9 (21-CH), 119.81, 119.85, 120.8, 121.0, 126.49, 126.52, 127.4, 127.48, 127.53, 127.6, 128.0, 128.1, 131.7, 131.8, 133.0, 133.1, 133.58, 133.63, 133.73, 133.78, 133.81, 133.86, 138.55, 133.59, 139.8, 140.6, 140.8, 144.86, 144.91, 162.70, 162.74, 174.24, 174.26, 193.16, 193.19. ^{1}H NMR (500 MHz, TFA-$CDCl_3$, monocations **27b,c**H^+): δ -2.03 (1H, s), 1.45-1.48 (3H, 2 overlapping triplets), 1.50-1.54 (3H, 2 overlapping triplets), 1.95 (6H, s), 3.02 (1H, br s), 3.17 (br s), 3.18 (br s) (1H), 3.44-3.49 (2H, m), 3.62-3.70 (2H, m), 4.32 (2H, s), 7.96 (1H, s), 8.08 (1H, s), 8.15-8.17 (1H, br d), 8.56-8.59 (1H, m), 9.02 (s), 9.04 (s) (1H), 9.61 (1H, s), 9.66 (s), 9.67 (s) (1H), 10.20 (1H, s). HRMS (ESI): *m/z* $[M + H]^+$ Calcd for $C_{34}H_{36}N_3O$ 502.2858; found 502.2861.

Computational Studies. All calculations were performed using Gaussian 09 Rev D.01 running on a Linux-based computer.[54] Energy minimization and frequency calculations of the porphyrinoid systems were performed at the density functional theory (DFT) level of theory with the B3LYP functional and the 6-311++G(d,p) triple-ζ basis set.[55-58] Single-point energy calculations were performed on the minimized structures using both the B3LYP-D3[59] and M062-X[60] functionals with a 6-311++G(d,p) triple-ζ basis set. The resulting Cartesian coordinates of the molecules can be found in Supporting Information.

Two types of NMR calculations were performed: the GIAO method with the B3LYP functional and a 6-31+G(d,p) basis set was used to obtain NICS values,[61] and CGST with the B3 functional and a 6-31+G(d,p) basis set to obtain AICD plots.[62] NICS(0) was calculated at the mean position of all four heavy atoms in the middle of the macrocycle. NICS(a), NICS(b), NICS(c), NICS(d), and NICS(e) values were obtained by applying the same method to the mean position of the heavy atoms that comprise the individual rings of each macrocycle. In addition, NICS(1)$_{zz}$, NICS(1a)$_{zz}$, NICS(1b)$_{zz}$, NICS(1c)$_{zz}$, NICS(1d)$_{zz}$, and NICS(1e)$_{zz}$ were obtained by applying the same

method to ghost atoms placed 1 Å above each of the corresponding NICS(0) points and extracting the zz contribution of the magnetic tensor. AICD for all the compounds were plotted, and these plots can also be found in Supporting Information.

ASSOCIATED CONTENT

Supporting Information

The Supporting Information is available free of charge on the ACS Publications website.

Tables giving Cartesian coordinates, calculated energies, selected bond lengths and AICD plots, and selected UV-Vis, ^{1}H NMR, ^{1}H-^{1}H COSY, HSQC, DEPT-135, $^{13}C\{^{1}H\}$ NMR, and mass spectra are provided (pdf).

AUTHOR INFORMATION

Corresponding Author

*E-mail: tdlash@ilstu.edu

ORCID

Timothy D. Lash: 0000-0002-0050-0385

Deyaa I. AbuSalim: 0000-0003-0813-0486

Notes

The authors declare no competing financial interest.

ACKNOWLEDGMENTS

This work was supported by the National Science Foundation under grants CHE-1465049 and CHE-1855240.

References

(1) Lindsey, J. S. *De Novo* Synthesis of Gem-Dialkyl Chlorophyll Analogues for Probing and Emulating Our Green World. *Chem. Rev.* **2015**, *115*, 6534-6620.

(2) Taniguchi, M.; Lindsey, J. S. Synthetic Chlorins, Possible Surrogates for Chlorophylls, Prepared by Derivatization of Porphyrins. *Chem. Rev.* **2017**, *117*, 344-535.

(3) Scheer, H. In *Chlorophylls*; Scheer, H, Ed.; CRC Press: Boca Raton, FL, 1991; pp 3-30.

(4) (a) Timkovich, R.; Cork, M. S.; Gennis, R. B.; Johnson, P. Y. Proposed structure of heme d, a prosthetic group of bacterial terminal oxidases *J. Am. Chem. Soc.* **1985**, *107*, 6069-6075. (b) Murshudov, G. N.; Grebenko, A. I.; Barynin, V.; Dauter, Z.; Wilson, K. S.; Vainshtein, B. K.; Melik-Adamyan, W.; Bravo, J.; Ferran, J. M.; Ferrer, J. C.; et al. Structure of the Heme d of *Penicillium vitale* and *Escherichia coli* Catalases. *J. Biol. Chem.* **1996**, *271*, 8863-8868.

(5) (a) Wang, W.; Kishi, Y. Synthesis and Structure of Tolyporphin A *O,O*-Diacetate. *Org. Lett.* **1999**, *1*, 1129-1132. (b) Bruckner, C. Tolyporphin – An Unusual Green Chlorin-like Dioxobacteriochlorin. *Photochem. Photobiol.* **2017**, *93*, 1320-1325.

(6) (a) Weeg-Aerssens, E.; Wu, W.; Ye, R. W.; Tiedje, J. M.; Chang, C. K. Purification of Cytochrome cdl Nitrite Reductase from Pseudomonas stutxeri JM300 and Reconstitution with Native and Synthetic Heme d_1. *J. Biol. Chem.* **1991**, **266**, 7496-7502. (b) Chang, C. K.; Wu, W. The Porphinedione Structure of Heme d_1. Synthesis and Spectral Properties of

Model Compounds of the Prosthetic Group of Dissimilatory Nitrite Reductase. *J. Biol. Chem.* **1986**, *261*, 8593-8596.

(7) Murphy, M. J.; Siegel, L. M.; Tove, S. R.; Kamin, H. Siroheme: A New Prosthetic Group Participating in Six-Electron Reduction Reactions Catalyzed by Both Sulfite and Nitrite Reductases. *Proc. Nat. Acad. Sci.* **1974**, *71*, 612-616.

(8) Ballantine, J. A.; Psaila, A. F.; Pelter, A.; Murray-Rust, P.; Ferrito, V.; Schembri, P.; Jaccarini, V. Structure of Bonellin and Its Derivatives. Unique Physiologically Active Chlorins from the Marine Echurian *Bonella Viridis*. *J. Chem. Soc., Perkin Trans. 1* **1980**, 1080-1089.

(9) (a) Pelter, A.; Ballantine, J. A.; Ferrito, V.; Jaccarini, V.; Psaila, A.; Schembri, P. J. Bonellin, a Most Unusual Chlorin. *J. Chem. Soc., Chem. Commun.* **1976**, 999-1000. (b) Dutton, C. J.; Fookes, C. J. R.; Battersby, A. R. Synthesis of the Chlorin Macrocycle by a Photochemical Approach. *J. Chem. Soc., Chem. Commun.* **1983**, 1237-1238. (c) Montforts, F.-P.; Schwartz, U. M. Total Synthesis of (±)-Bonellin Dimethyl Ester. *Angew. Chem. Int. Ed. Engl.* **1985**, *24*, 775-776.

(10) (a) Karuso, P.; Berquist, P. R.; Buckleton, J. S.; Cambie, R. C.; Clark, G. R.; Richard, C. E. F. 13^2,17^3-Cyclopheophorbide Enol, the First Porphyrin Isolated from a Sponge. *Tetrahedron Lett.***1986**, *27*, 2177-2178. (b) Schopf, J. W. In *Earth's Earliest Biosphere: Its Origin and Evolution*; Schopf, J. W., Ed.; Princeton University Press: Princeton, 1983; p 543. (c) Bible, K. C.; Buyendorp, M.; Zierath, P. D.; Rinehart, K. L. Tunichlorin: a Nickel Chlorin Isolated from the Caribbean Tunicate *Trididemnum Solidum*. *Proc. Natl. Acad. Sci.* **1988**, *85*, 4582-4586. (d) Sakata, K.; Yamamoto, K.; Ishikawa, H.; Yagi, A.; Etoh, H.; Ina, K. Chlorophyllone-a, a New Pheophorbide-*a* related Compound Isolated from *Ruditapes*

Philippinarum as an Antioxidative Compound. *Tetrahedron Lett.* **1990**, *31*, 1165-1168. (e) Yamamoto, K.; Sakata, K.; Watanabe, N.; Yagi, A.; Brinen, L. S.; Clardy, J. Chlorophyllonic Acid and Methyl Ester, a New Chlorophyll *a* Related Compound Isolated as an Antioxidant from Short-Necked Clam, *Ruditapes Philippinarum*. *Tetrahedron Lett.* **1992**, *33*, 2587-2588. (f) Watanabe N., Yamamoto K., Ishikawa H., Yagi A., Sakata K., Brinen L. S., and Clardy J. New Chlorophyll-*a* Related Compounds Isolated as Antioxidants from Marine Bivalves. *J. Nat. Prod.* **1993**, *56***,** 305–317. (g) Dolphin, D.; Ma, L. Stereoselective Synthesis of New Chlorophyll *a* Related Antioxidants Isolated from Marine Organisms. *J. Org. Chem.* **1996**, *61*, 2501-2510.

(11) (a) Scott, L. J.; Goa, K. L. Verteporfin. *Drugs & Aging* **2000**, *16*, 139-146. (b) Karim, S. P.; Adelman, R. A. Profile of Vertiporpfin and Its Potential for the Treatment of Central Serious Chorioretinopathy. *Clin. Ophthalmol.* **2013**, *7*, 1867-1875. (c) Ethirajan, M.; Chen, Y.; Joshi, P.; Pandey, R. K. The Role of Porphyrin Chemistry in Tumor Imaging and Photodynamic Therapy. *Chem. Soc. Rev.* **2011**, *40*, 340-362.

(12) Jain, M.; Zellweger, M.; Frobert, A.; Valentin, J.; van den Bergh, H.; Wagnieres, G.; Cook, S.; Giraud, M.-N. Intra-Arterial Drug and Light Delivery for Photodynamic Therapy Using Visodyne®: Implication for Atherosclerotic Plaque Treatment. *Front. Physiol.* **2016**, *7*, 400.

(13) (a) Senge, M. O.; Brandt, J. C. Temoporfin (Foscan®, 5,10,15,20-tetra(*m*-hydroxyphenyl)chlorin) - a second-generation photosensitizer. *Photochem. Photobiol.* **2011**, *87*, 1240-1296. (b) Senge, M. O. *Photodiagnosis Photodyn. Ther.* 2012, *9*, 170. (c) de Visscher, S. A.; Dijkstra, P. U.; Tan, I. B.; Roodenburg, J. L.; Witjes, M. mTHPC

Mediated Photodynamic Therapy (PDT) of Squamous Cell Carcinoma in the Head and Neck: a Systematic Review. *J. Oral Oncol.* 2013, *49*, 192.

(14) (a) Wang, S.; Bromley, E.; Xu, L.; Chen, J. C.; Keltner, L. Talaporfin Sodium. *Expert Opin. Pharmacother.* **2010**, *11*, 133-140. (b) Miki, Y.; Akimoto, J.; Hiranuma, M.; Fujiwara, Y. Effect of talaporfin sodium-mediated photodynamic therapy on cell death modalities in human glioblastoma T98G cells. *J. Toxicol. Sci.* **2014**, *39*, 821-827.

(15) Liu, Y.; Zhang, S.; Lindsey, J. S. Total Synthesis Campaigns Towards Chlorophylls and Related Natural Hydroporphyrins – Diverse Macrocycles, Unrealized Opportunities. *Nat. Prod. Rep.* **2018**, *35*, 879-901.

(16) (a) Callot, H. J.; Schaeffer, E. Homologation Directe du Cycle des Porphyrines par les Diazoalcanes. *Tetrahedron* **1978**, *34*, 2295−2300. (b) Vogel, E.; Kocher, M.; Balchi, M.; Teichler, I.; Lex, J.; Schmickler, H.; Ermer, O. 2,3-Dihydroporphycene – an Analogue of Chlorin. *Angew. Chem., Int. Ed. Engl.* **1987**, *36*, 931-934. (c) McCarthy, J. R.; Jenkins, H. A.; Brückner, C. Free Base *meso*-Tetraaryl-morpholinochlorins and Porpholactone from *meso*-Tetraaryl-2,3-dihydroxy-chlorin. *Org. Lett.* **2003**, *5*, 19-22. (d) Lara, K. K.; Rinaldo, C. R.; Brückner, C. *meso*-Tetraaryl-7,8-dihydroxydithiachlorins: First Examples of Heterochlorins. *Tetrahedron Lett.* **2003**, *44*, 7793-7796. (e) Akhigbe, J.; Haskoor, J.; Krause, J. A.; Zeller, M.; Brückner, C. Formation, Structure, and Reactivity of *meso*-Tetraaryl-chlorolactones, -porpholactams, and –chlorolactams, Porphyrin and Chlorin Analogues Incorporating Oxazolone or Imidazolone Moieties. *Org. Biomol. Chem.* **2013**, *11*, 3616-3628. (f) Ogikubo, J.; Meehan, E.; Engle, J. T.; Ziegler, C. J.; Bruckner, C. *meso*-Aryl-3-alkyl-2-oxachlorins. *J. Org. Chem.* **2012**, *77*, 6199-6207.

(17) Lash, T. D. Carbaporphyrinoid Systems. *Chem. Rev.* **2017**, *117*, 2313−2446.

(18) Lash, T. D. Metal Complexes of Carbaporphyrinoid Systems. *Chem. Asian J.* **2014**, *9*, 682-705.

(19) Hayes, M. J.; Lash, T. D. Carbachlorins. *Chem. Eur. J.* **1998**, *4*, 508-511.

(20) Li, D.; Lash, T. D. Synthesis and Reactivity of Carbachlorins and Carbaporphyrins. *J. Org. Chem.* **2014**, *79*, 7112-7121.

(21) Navneet, S.; Ferrence, G. M.; Lash, T. D. Synthesis and Properties of Carbaporphyrin and Carbachlorin Dimethyl Esters Derived from Cyclopentanedialdehydes. *J. Org. Chem.* **2017**, *82*, 9715-9730.

(22) Li, D.; Lash, T. D. Synthesis and Oxidation of Internally Chlorinated Carbachlorins. *Eur. J. Org. Chem.* **2017**, 6775-6780.

(23) Lash, T. D. Out of the Blue! Azuliporphyrins and Related Carbaporphyrinoid Systems. *Acc. Chem. Res.* **2016**, *49*, 471-482.

(24) Lash, T. D.; Colby, D. A.; Graham, S. R.; Ferrence, G. M.; Szczepura, L. F. Organometallic Chemistry of Azuliporphyrins: Synthesis, Spectroscopy, Electrochemistry and Structural Characterization of Nickel(II), Palladium(II) and Platinum(II) Complexes of Azuliporphyrins. *Inorg. Chem.* **2003**, *42*, 7326−7338.

(25) Bialek, M.; Latos-Grazyński, L. Merging of Inner and Outer Ruthenium Organometallic Coordination Motifs Within an Azuliporphyrin Framework. *Chem. Commun.* **2014**, *50*, 9270−9272.

(26) Stateman, L. M.; Ferrence, G. M.; Lash, T. D. Rhodium(III) Azuliporphyrins. *Organometallics* **2015**, *34*, 3842−3848.

(27) Lash, T. D.; Pokharel, K.; Zeller, M.; Ferrence, G. M. Iridium(III) Azuliporphyrins. *Chem. Commun.* **2012**, *48*, 11793− 11795.

(28) Lash, T. D.; Chaney, S. T. Azuliporphyrin, a Case of Borderline Porphyrinoid Aromaticity. *Angew. Chem., Int. Ed. Engl.* **1997**, *36*, 839− 840.

(29) Lash, T. D.; Colby, D. A.; Graham, S. R.; Chaney, S. T. Synthesis, Spectroscopy, and Reactivity of *meso*-Unsubstituted Azuliporphyrins and Their Heteroanalogues. Oxidative Ring Contractions to Carba-, Oxacarba-, Thiacarba-, and Selenacarbaporphyrins. *J. Org. Chem.* **2004**, *69*, 8851-8864.

(30) Larsen, S.; McCormick-McPherson, L. J.; Teat, S. J.; Ghosh, A. *ACS Omega* **2019**, *4*, 6737-6745.

(31) Richter, D. T.; Lash, T. D. Synthesis of Sapphyrins, Heterosapphyrins, and Carbasapphyrins by a "4 + 1" Approach. *J. Org. Chem.* **2004**, *69*, 8842-8850.

(32) Sasaki, Y.; Takase, M.; Okujima, T.; Mori, S.; Uno, H. Synthesis and Redox properties of Pyrrole- and Azulene-Fused Azacoronene. *Org. Lett.* **2019**, *21*, 1900-1903.

(33) Results presented in part at the *255th ACS National Meeting*, New Orleans, LA, March 18-22, 2018. Abstract: Noboa, M. A.; Lash, T. D. Investigations Directed Towards the Synthesis of Carbachlorins. *Abstracts of Papers*, ORGN-633.

(34) Lash, T. D. What's in a Name? The MacDonald Condensation. *J. Porphyrins Phthalocyanines* **2016**, *20*, 855-888.

(35) Jacobi, P. A.; Lanz, S.; Ghosh, I.; Leung, S. H.; Lower, F.; Pippen, D. A New Synthesis of Chlorins. *Org. Lett.* **2001**, *3*, 831-834.

(36) O'Neal, W. G.; Roberts, W. P.; Ghosh, I.; Jacobi, P. A. Studies of Chlorin Chemistry. II. A Versatile Synthesis of Dihydrodipyrrins. *J. Org. Chem.* **2005**, *70*, 7243-7251.

(37) O'Neal, W. G.; Robert, W. P.; Ghosh, I.; Wang, H.; Jacobi, P. A. Studies in Chlorin Chemistry. 3. A Practical Synthesis of C,D-Ring Symmetric Chlorins of Potential Utility in Photodynamic Therapy. *J. Org. Chem.* **2006**, *71*, 3472-3480.

(38) O'Neal, W. G.; Jacobi, P. A. Towards a General Synthesis of Chlorins. *J. Am. Chem. Soc.* **2008**, *130*, 1102-1108.

(39) Liu, Y.; Allu, S.; Reddy, M. N.; Hood, D.; Diers, J. R.; Bocian, D. F.; Holten, D.; Lindsey, J. S. Synthesis and Photophysical Characterization of Bacteriochlorins Equipped with Integral Swallowtail Substituents. *New J. Chem.* **2017**, *41*, 4360-4376.

(40) Lash, T. D.; Lammer, A. D.; Idate, A. S.; Colby, D. A.; White, K. Preparation of Azulene-Derived Fulvenedialdehydes and Their Application to the Synthesis of Stable *adj*-Dicarbaporphyrinoids. *J. Org. Chem.* **2012**, *77*, 2368-2381.

(41) Lash, T. D.; El-Beck, J. A.; Ferrence, G. M. Synthesis and Reactivity of *meso*-Unsubstituted Azuliporphyrins Derived from 6-*tert*-Butyl- and 6-Phenylazulene. *J. Org. Chem.* **2007**, *72*, 8402-8415.

(42) Lash, T. D. The Azuliporphyrin-Carbaporphyrin Connection. *Chem. Commun.* **1998**, 1683-1684.

(43) Colby, D. A.; Lash, T. D. Adaptation of the Rothemund Reaction for Carbaporphyrin Synthesis: Preparation of *meso*-Tetraphenylazuliporphyrin and Related Benzocarbaporphyrins. *Chem. Eur. J.* **2002**, *8*, 5397-5402.

(44) Lash, T. D.; Hayes, M. J.; Spence, J. D.; Muckey, M. A.; Ferrence, G. M.; Szczepura, L. F. Conjugated Macrocycles Related to the Porphyrins. 21. Synthesis, Spectroscopy, Electrochemistry, and Structural Characterization of Carbaporphyrins. *J. Org. Chem.* **2002**, *67*, 4860-4874.

(45) Grabowski, E. Y.; AbuSalim, D. I.; Lash, T. D. Naphtho[2,3-*c*]carbaporphyrins. *J. Org. Chem.* **2018**, *83*, 11825-11838.

(46) (a) Ghosh, A. First-principles Quantum Chemical Studies of Porphyrins. *Acc. Chem. Res.* **1998**, *31*, 189−198. (b) Ghosh, A. Quantum Chemical Studies of Molecular Structures and Potential Energy Surfaces of Porphyrins and Hemes. *The Porphyrin Handbook*; Kadish, K. M.; Smith, K. M.; Guilard, R., Eds.; Academic Press: San Diego, 2000; Vol. 7, pp 1−38.

(47) Alonso, M.; Geerlings, P.; De Proft, F. Exploring the Structure- Aromaticity Relationship in Hückel and Möbius N-Fused Pentaphyrins using DFT. *Phys. Chem. Chem. Phys.* **2014**, *16*, 14396−14407.

(48) Alonso, M.; Geerlings, P.; De Proft, F. Topology Switching in [32]Heptaphyrins Controlled by Solvent, Protonation, and *meso* Substituents. *Chem. - Eur. J.* **2013**, *19*, 1617−1628.

(49) Schleyer, P. v. R.; Maerker, C.; Dransfeld, A.; Jiao, H.; van Eikema Hommes, N. J. R. Nucleus-Independent Chemical Shifts: a Simple and Efficient Aromaticity Probe. *J. Am. Chem. Soc.* **1996**, *118*, 6317−6318.

(50) Geuenich, D.; Hess, K.; Köhler, F.; Herges, R. Anisotropy of Induced Current Density (ACID), a General Method to Quantify and Visualize Electronic Delocalization. *Chem. Rev.* **2005**, *105*, 3758− 3772.

(51) AbuSalim, D. I.; Lash, T. D. Tropylium and Porphyrinoid Character in Carbaporphyrinoid Systems. Relative Stability and Aromatic Characteristics of Azuliporphyrin and Tropiporphyrin Tautomers, Protonated Species, and Related Structures. *J. Phys. Chem. A* **2019**, *123*, 230-246.

(52) Jayasundera, K. P.; Kinoshita, H.; Inomata, K. An Efficient Method to Construct the A,B-

Rings Component toward Total Syntheses of and Its Derivative as a Photoprobe. *Bull. Chem. Soc. Jpn.* **2000**, *73*, 497-505.

(53) Clezy, P. S.; Crowley, R. J.; Hai, T. T. The Chemistry of Pyrrolic Compounds. L. The Synthesis of Oxorhodoporphyrin Dimethyl Ester and Some of Its Derivatives. *Aust. J. Chem.* **1982**, *35*, 411-421.

(54) Frisch, M. J.; Trucks, G. W.; Schlegel, H. B.; Scuseria, G. E.; Robb, M. A.; Cheeseman, J. R.; Scalmani, G.; Barone, V.; Petersson, G. A.; Nakatsuji, H.; et al. *Gaussian 09, Revision D.01*; Gaussian, Inc., Wallingford, CT, 2016.

(55) Becke, A. D. Density Functional Thermochemistry. III. The Exact Role of Exchange. *J. Chem. Phys.* **1993**, *98*, 5648−5652.

(56) Lee, C.; Yang, W.; Parr, R. G. Development of the Colle-Solvetti Correlation-Energy Formula into a Functional of the Electron Density. *Phys. Rev. B: Condens. Matter Mater. Phys.* **1988**, *37*, 785− 789.

(57) Vosko, S. H.; Wilk, L.; Nusair, M. Accurate Spin-Dependent Electron Liquid Correlation Energies for Local Spin Density Calculations: A Critical Analysis. *Can. J. Phys.* **1980**, *58*, 1200−1211.

(58) Stephens, P. J.; Devlin, F. J.; Chabalowski, C. F.; Frisch, M. J. *Ab Initio* Calculations of Vibrational Absorption and Circular Dichroism Spectra using Density Functional Force Fields. *J. Phys. Chem.* **1994**, *98*, 11623−11627.

(59) Grimme, S.; Antony, J.; Ehrlich, S.; Krieg, H. A Consistent and Accurate Ab Initio Parametrization of Density Functional Dispersion Correction (DFT-D) for the 94 Elements H-Pu. *J. Chem. Phys.* **2010**, *132*, 154104.

(60) Zhao, Y.; Truhlar, D. G. The M06 Suite of Density Functionals for Main Group

Thermochemistry, Thermochemical Kinetics, Noncovalent Interactions, Excited States, and Transition Elements: Two New Functionals and Systematic Testing of Four M06-Class Functionals and 12 Other Functionals. *Theor. Chem. Acc.* **2008**, *120*, 215−241.

(61) Wolinski, K.; Hinton, J. F.; Pulay, P. Efficient Implementation of the Gauge-independent Atomic Orbital Method for NMR Chemical Shift Calculations. *J. Am. Chem. Soc.* **1990**, *112*, 8251−8260.

(62) Herges, R.; Geuenich, D. Delocalization of Electrons in Molecules. *J. Phys. Chem. A* **2001**, *105*, 3214−3220.